ADDIS ABABA UNIVERSITY
SCHOOL OF GRADUATE STUDIES
FACULTY OF TECHNOLOGY
ELCTRICAL AND COMPUTER ENGINEERING DEPARTMENT

ANALYSIS AND DESIGN OF A COMPACT MICROSTRIP PATCH ANTENNA WITH ENHANCED BANDWIDTH AND GAIN FOR WIRELESS LOCAL AREA NETWORK (WLAN) COMMUNICATIONS

BY
FEYISA DEBO

A thesis submitted to school of Graduate Studies of Addis Ababa University in partial fulfillment of

Masters of Science
In
Electrical Engineering (Communication Engineering)

Date: July, 2010
Addis Ababa, Ethiopia

ADDIS ABABA UNIVERSITY
SCHOOL OF GRADUATE STUDIES
FACULTY OF TECHNOLGY
ELECTRICAL AND COMPUTERENGINEERING
DEPARTMENT

ANALYSIS AND DESIGN OF A COMPACT MICROSTRIP PATCH ANTENNA WITH ENHANCED BANDWIDTH AND GAIN FOR WIRELESS LOCAL AREA NETWORK (WLAN) COMMUNICATIONS

BY
FEYISA DEBO

Advisor
Dr. Ing. Mohammed Abdo

ADDIS ABABA UNIVERSITY

SCHOOL OF GRADUATE STUDIES

FACULTY OF TECHNOLGY

ELECTRICAL AND COMPUTER ENGINEERING

ANALYSIS AND DESIGN OF A COMPACT MICROSTRIP PATCH ANTENNA WITH ENHANCED BANDWIDTH AND GAIN FOR WIRELESS LOCAL AREA NETWORK (WLAN) COMMUNICATIONS

BY

FEYISA DEBO

APPROVAL BY BOARD OF EXAMINERS

_____	_____
Chairman Dept. of Graduate Committee	Signature
Dr. Ing. Mohammed Abdo	_____
Advisor	Signature
_____	_____
Internal Examiner	Signature
_____	_____
External Examiner	*Signature*

ACKNOWLEDGEMENTS

I would like to express my sincere gratitude to my advisor, Dr. Ing.Mohammed Abdo for his generous support, comments, advice and guidance throughout the duration of my thesis. Because of his broad research interest, he encouraged me to explore interesting properties of different microstrip patch antennas.

Special thanks to Ato Esuballew Abayneh for his corporative guidance and all my friends who have provided assistance at various occasions.., thanks for being such a wonderful companion.

Lastly I would like to thank my mother for her prayer and inspiration which has helped me for successful completion of the study.

TABLE OF CONTENTS

CHAPTER 5

CONCLUSION AND RECOMANDATIONS FOR FUTURE WORK

LIST OF TABLES

LIST OF FIGURES

v

List of Constants and Symbols

$c=3X10^{8}$ meters/second — c= velocity of wave in free space

$_{0}=\frac{1}{36}\boldsymbol{X}10^{-12}$ Farads/meter — ε_0=permittivity of free space

$\mu_0=4\ \boldsymbol{X}10^{-7}$ Henry/meter — μ_0 =permeability of free space

ε_r = relative permittivity

μ_r= relative permeability

List of Acronyms

BW .....Bandwidth

DBS.....Direct Broadcast Satellites

FDTD.....Finite Difference Time Domain Method

GPS.....Global Position Satellites

MoM.....Method of Moments

MMIC.....Monolithic Microwave Integrated Circuits

MSA..... Microstrip Antenna

RF..... Radio Frequency

RL..... Return Loss

SWR .....Standing Wave Ratio

TL.....Transmission Line

VSWR.....Voltage Standing Wave Ratio

WLAN.....Wireless Local Area Networks

3D .....Three Dimension

ABSTRACT

In this thesis, the compact microstrip patch antennas in stacked configuration have been proposed. The microstrip patch antenna structure consists of a square patch with four equal u-shape on four sides of each patches. These structures provide an optimized patch area resulting in a substantial reduction in size compared to a typical microstrip square patch designed at the same frequency of operation. The characteristics of the antenna are obtained in terms of return loss, gain, radiation pattern and bandwidth and are compared with the conventional microstrip patch. The stacked configuration enhances both gain and bandwidth of the microstrip patch antenna at 2.45GHZ operating frequency. A size reduction of 70% is obtained along width 24.4dB gain and 6.6519GHZ bandwidth. The empire software is used to obtain the optimized performance of the proposed antenna. This antenna is found to be suitable for WLAN communications.

Key Words: *size reduction, stacked microstrip patch antenna, gain, bandwidth.*

CHAPTER 1

1.1 INTRODUCTION

Rapid progress in wireless communication promises to replace wired communication networks in which antennas play a key important role. In the last few years, the development of wireless local area networks (WLAN) represented one of the principal interests in the information and communication field. Thus, the current trend in commer develop capable frequen design c

Micro exhibite easy fab to the c while n that lin antenna antenna be decr

and bandwidth enhancement has become a major consideration in the microstrip antenna design. Many studies have been carried out and several proposed techniques are proven to be able to reduce the size of the patch and to improve the bandwidth and gain of the microstrip antenna [1][2][6][7][12].

In this work, applying **u** shape on four sides of square microstrip patch antenna a significant size reduction is obtained. However size reduction comes at the cost of bandwidth and gain which is then enhanced to a good level using stacked configuration on a reduced size microstrip patch antenna. Owing to the fact that stacked configuration technique enhances both the gain and bandwidth; this particular choice is preferred in the present work.

1.2 Objectives

The objective of the thesis is to design and analyze the compact microstrip antennas with enhanced bandwidth and gain using stacked configuration and to compare the stacked microstrip antennas with conventional microstrip antennas in terms of bandwidth, gain and size of the antennas. The antennas are operating at 2.45GHZ and it is excited by lumped port and inset feeding techniques.

1.3 Literature Review

A number of researches have been carried out to enhance the bandwidth, gain or to reduce the size of microstrip patch antenna separately but not comprehensively all at once. For example in,[4] the objective was to achieve a wide operating bandwidth of microstrip patch antenna regardless of size reduction and suggested for future development the miniaturization of microstrip patch antenna with out loss of efficiency. In [5] the objective was only stacking microstrip patch antenna configuration to achieve dual or multiple frequency operation. On the other hand, [6] examines the reduction of antenna size with less focus on bandwidth and gain. Throughout the years, authors have dedicated their investigations to create new designs or variations to the original antenna that, to some extent; produce either

wider bandwidths or multiple-frequency operation in a single element not in stacked arrangement. However, most of these innovations bear disadvantages related to the size. The improvement in bandwidth suffers usually from a degradation of the other characteristics. It is the aim of this thesis to design and analyze a microstrip patch antenna with improved bandwidth, gain and reduced size all in one. Achieving these three goals at the same time is believed to be the main contribution of this work.

1.3 Outline of the Thesis

The thesis comprises of five chapters and the overview of each chapter as follows:

Chapter 1: This chapter provides the introduction, objective and literature reviews on microstrip antenna.

Chapter 2: Chapter 2 presents the microstrip antenna basic parameters, the feeding methods and the methods of analysis that can be used for the microstrip antenna design.

Chapter 3: This chapter explains the analysis and design of conventional and stacked microstrip antennas.

Chapter 4: The simulation and results obtained are discussed in this chapter.

Chapter 5: Conclusion of the thesis and suggestions for future work are presented in this final chapter.

CHAPTER 2

MICROSTRIP PATCH ANTENNA

2.1 Introduction

Microstrip patch antennas were first proposed In the 1970s and since then a massive amount of research and development efforts have been put into it. This phenomenon has been accelerated due to its advantages over other antennas' structures, which includes: [1]

i. Lightweight, low volume and thin profile configuration, making them easily incorporated into any package.
ii. Low profile planar configuration that can be easily made conformal to host surface.
iii. Low fabrication cost, hence can be manufactured in large quantities.
iv. Supports both, linear as well as circular polarization.
v. Can be easily integrated with microwave integrated circuits (MICs).
vi. Capable of dual and triple frequency operations and provides flexibility to be constructed in any shape.
vii. Mechanically robust when mounted on rigid surfaces.

On the other hand, there are also some limitations compared to the conventional microwave antennas .These are:-

i. Narrow bandwidth
ii. Relatively poor radiation efficiency
iii. Low gain and inherently low directivity

iv. High losses resulting from surface wave excitation and conductor and dielectric losses.

V. Difficult to analyze - Typically a full-wave computationally intensive numerical analysis is required.

2.2 Basic Patch Antenna Shapes and Geometries

In its most basic form, a microstrip patch antenna consists of a radiating patch on one side of a dielectric substrate, which has a ground plane on the other side as shown in Figure 2.1

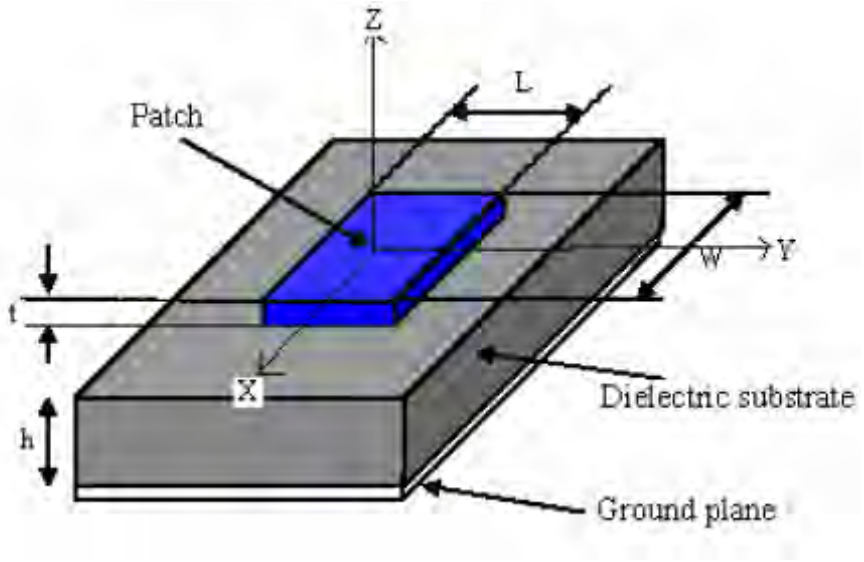

Figure 2.1: Structure of a microstrip patch antenna.

The patch is generally made of conducting material such as copper or gold and can take any possible shape. The radiating patch and the feed lines are usually photo etched on the dielectric substrate.

In order to simplify analysis and performance prediction, the patch is generally square, rectangular, circular, triangular, elliptical or some

other common shapes as shown in Figure 2.2.However, the conventional square, rectangular and circular MSAs are the most popular because of simple fabrication, performance prediction and analysis, besides their attractive radiation characteristics such as low cross-polarization radiation.

Circular and elliptical shapes are slightly smaller than rectangular patches. Thus they will have smaller bandwidth and gain. The circular geometry patches are difficult to analyze due to their inherent geometry.

Triangular patch is even smaller than both rectangular and circular geometries. However, this will produce even lower gain and smaller bandwidth. It will also produce higher cross-polarization due to its unsymmetrical geometry. Dual polarized patch could be generated from these geometries.

Circular ring patches have relatively the smallest conductor size, but at the expense of bandwidth and gain. Furthermore, for this geometry, it will not be easy to excite lower order modes and obtain a good impedance match for resonance. Non-contacting forms of excitation are normally used for this shape.

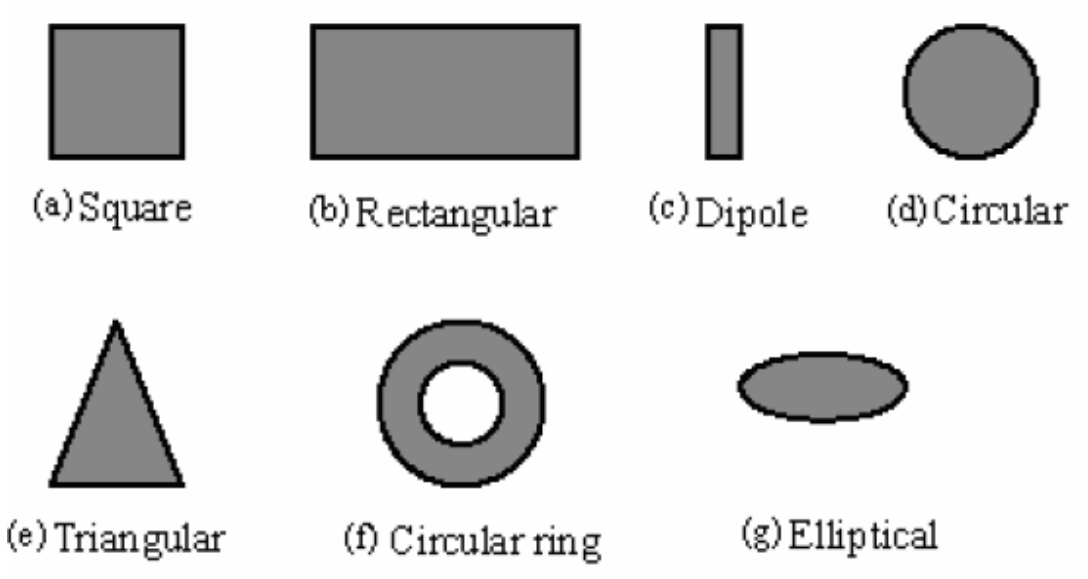

Figure 2.2: Common shapes of microstrip patch elements.(1)

2.3 Microstrip Antenna Feed Techniques

Microstrip patch antennas can be fed by a variety of methods. These methods can be classified into two categories- contacting and non-contacting. In the contacting method, the RF power is fed directly to the radiating patch using a connecting element such as a microstrip line. In the non-contacting scheme, electromagnetic field coupling is done to transfer power between the microstrip line and the radiating patch.

2.3.1 Microstip Line Feed (Inset Feed)

In this type of feed technique, a conducting strip is connected directly to the edge of the microstrip patch as shown in Figure 2.3. The conducting strip is smaller in width as compared to the patch and this kind of feed arrangement has the advantage that the feed can be etched on the same substrate to provide a planar structure[1].

The purpose of the inset cut in the patch is to match the impedance of the feed line to the patch without the need for any additional matching element. This is achieved by properly controlling the inset position. Hence this is an easy feeding scheme, since it provides ease of fabrication and simplicity in modeling as well as impedance matching. However as the thickness of the dielectric substrate being used, increases, surface waves and spurious feed radiation also increases, which hampers the bandwidth of the antenna. The feed radiation also leads to undesired cross-polarized radiation.

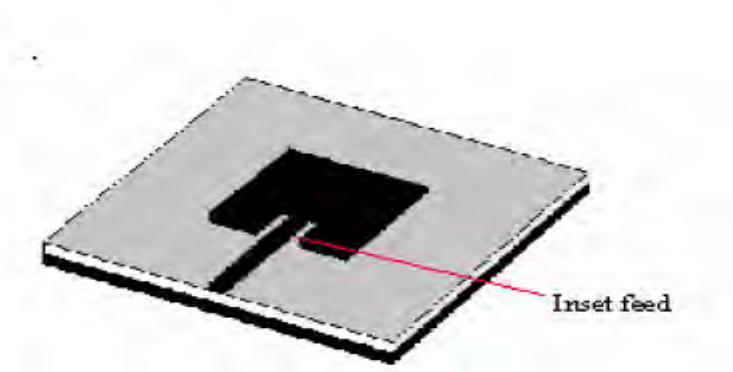

Figure 2.3: Direct contact microstrip feed line

2.3.2 Coaxial Probe Feed

The Coaxial feed or probe feed is a very common technique used for feeding microstrip patch antennas. As seen from Figure 2.4, the inner conductor of the coaxial connector extends through the dielectric and is soldered to the radiating patch, while the outer conductor is connected to the ground plane.

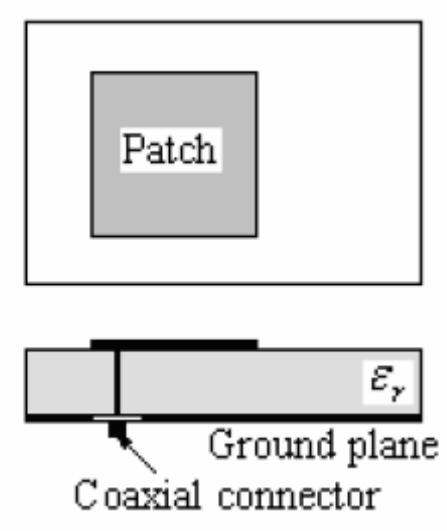

Figure 2.4 Probe fed microstrip patch antenna

The main advantage of this type of feeding scheme is that the feed can be placed at any desired location inside the patch in order to match with its input impedance. This feed method is easy to fabricate and has low spurious radiation. However, its major disadvantage is that it provides narrow bandwidth and is difficult to model since a hole has to be drilled in the substrate and the connector protrudes outside the ground plane, thus not making it completely planar for thick substrates ($h > 0.02\ _0$). Also, for thicker substrates, the increased probe length makes the input impedance more inductive, leading to matching problems [3]. Consequently for a thick dielectric substrate, which provides broad bandwidth, the microstrip line feed and the coaxial feed suffer from numerous disadvantages such as spurious feed radiation and matching problem. The non-contacting feed techniques which have been discussed below, solve these problems.

2.3.3 Aperture Coupled Feed

In this type of feed technique, the ground plane as shown in Figure 2.5 separates the radiating patch and the microstrip feed line. Coupling between the patch and the feed line is made through a slot or an aperture in the ground plane.

The coupling aperture is usually centered under the patch, leading to lower cross polarization due to symmetry of the configuration. The amount of coupling from the feed line to the patch is determined by the shape, size and location of the aperture. Since the ground plane separates the patch and the feed line, spurious radiation is minimized. Generally, a high dielectric material is used for the bottom substrate and a thick, low dielectric constant material is used for the top substrate to optimize radiation from the patch [1]. The major disadvantage of this feed technique is that it is difficult to fabricate due to multiple layers, which also increases the antenna thickness. This feeding scheme also provides narrow bandwidth.

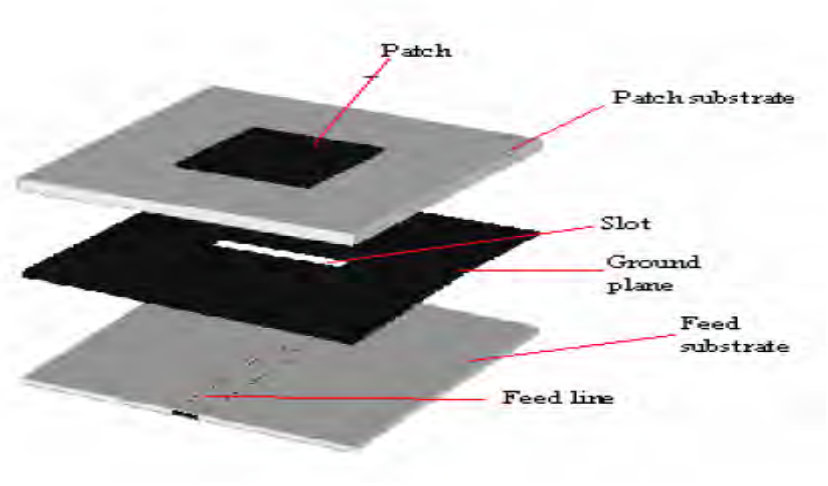

Figure2. 5 Aperture coupled Microstrip patch antenna

2.3.4 Proximity Coupled Feed

This type of feed technique is also called as the electromagnetic coupling scheme. As shown in Figure 2.6, two dielectric substrates are used such that the feed line is between the two substrates and the radiating patch is on top of the upper substrate. The main advantage of this feed technique is that it eliminates spurious feed radiation and provides very high bandwidth (as high as 13%) [4], due to overall increase in the thickness of the microstrip patch antenna. This scheme also provides choices between two different dielectric media, one for the patch and one for the feed line to optimize the individual performances**.**

Matching can be achieved by controlling the length of the feed line and the width-to-line ratio of the patch. The major disadvantage of this feed scheme is that it is difficult to fabricate because of the two dielectric layers that need proper alignment. Also, there is an increase in the overall thickness of the antenna.

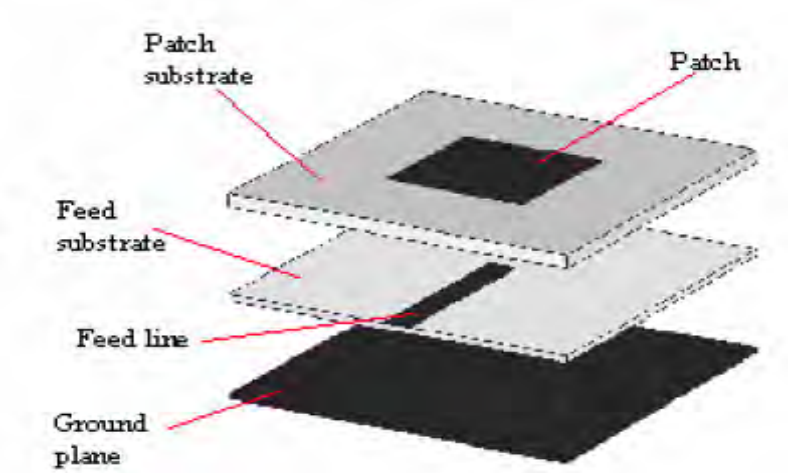

Figure 2.6 proximity coupled microstrip antenna

2.4 Methods of Analysis

The most popular models for the analysis of Microstrip patch antennas are the transmission line model, cavity model, and full wave model (which include primarily integral equations/Moment Method) [1]. The transmission line model is the simplest of all and it gives good physical insight but it is less accurate. The cavity model is more accurate and gives good physical insight but is complex in nature. The full wave models are extremely accurate, versatile and can treat single elements, finite and infinite arrays, stacked elements, arbitrary shaped elements and coupling. These give less physical insight as compared to the two models mentioned above and are far more complex in nature.

2.4.1. Transmission Line Model (TL)

Transmission line model is the easiest of all but it yields the least accurate results and it lacks the versatility. However it does shed some physical insight. As shown in Figure 2.7, we can represent a rectangular patch antenna with two narrow radiating apertures (slots), each slot of width W and height h and separated by a low impedance transmission line with a length equal to that of the patch antenna L and with characteristic impedance Z_{01}, where $Z_{01}=\frac{1}{Y_{01}}$. ($\frac{1}{Y_{01}}$ is the characteristic admittance).

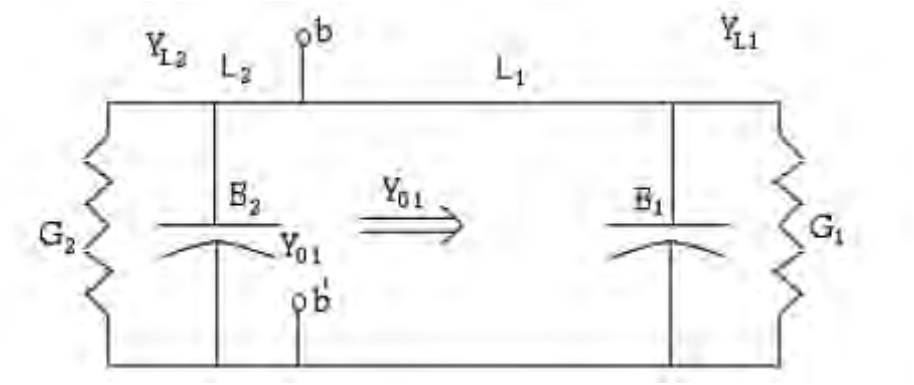

Figure 2.7: Transmission line model for rectangular MSA

In this model $\boldsymbol{Y_{L1}}$ and Y_{L2} represents the radiating apertures on the edges of the patch antenna, and because they are identical, we get

$$\boldsymbol{Y_{L1}} = G1 + JB_1 = Y_{L2} = G_2 + jB_2$$
$$B_1 = B_2,\ G_1 = G_2 \qquad (2.1)$$

where G_1, G_2 are the aperture conductancess and B_1, B_2 are the aperture susceptances. Approximate values of $G1$, G_2 and B_1, B_2 can be computed as follows [13].

$$G_1 = G_2 = 0.00836\frac{\boldsymbol{W}}{\lambda_0}$$

$$and\ B1 = B_2 = 0.01668\frac{\Delta \boldsymbol{L}}{\boldsymbol{h}}\frac{\boldsymbol{W}}{\lambda_0} \qquad \varepsilon_{reff} \qquad (2.2)$$

where W is the width of a rectangular MSA, ΔL is *defined in equation (2.7) which is* the length extension, h is the thickness (height) of the dielectric substrate, ε_{reff} is the effective dielectric constant and λ_0 is the wavelength in free space. The input feed point for the signal must

be placed in such a point along the transmission line where the input impedance matches 50 Ω and the antenna reactance minimized as much as possible.

At the signal feed point, the input admittance $Y_{bb.}$ Is given by [7]:

$$Y_{bb} = Y_{01}\left(\frac{Y_L + jY_{01}\tan(\quad_1)}{Y_{01} + jY_L\tan(\quad_1)} + \frac{Y_L + jY_{01}\tan(\quad_2)}{Y_{01} + jY_L\tan(\quad_2)}\right) \quad (2.3)$$

The optimal width of a rectangular MSA can be found as follows [1]

$$W = \frac{1}{2f_r\sqrt{\quad_o\ \quad_o}}\sqrt{\frac{2}{\quad_r+1}} = \frac{c}{2f_r}\sqrt{\frac{2}{\quad_r+1}} \quad (2.4)$$

Where c is the free-space velocity of light ($c \approx 3\times10^8$ m/s), f_0 is the resonance (operating) frequency and ε_r is the dielectric coefficient of the substrate. Because of fringing phenomena, where some waves travel in the substrate and some in the air as shown in Figure 2.8, the effective dielectric constant ε_{eff} is defined. On the edges of the patch antenna, fringing electric fields affect the electrical length of the MSA. Thus, it affects the resonance frequency of the MSA, so it must be taken into account. The same applies to the width.

In fact, the patch is electrically a bit larger than its physical dimensions due to fringing fields. The deviation between the electrical and physical size is dependent on both dielectric constant and height.

In general, fringing is a function of the ratio of the length of the patch, L to the height of the substrate h (L/h), and the dielectric coefficient of the substrate ε_r .The resonance frequency is influenced by ground plane size, dielectric height and patch width. So we have to find the actual length that would give the same desired resonance frequency.

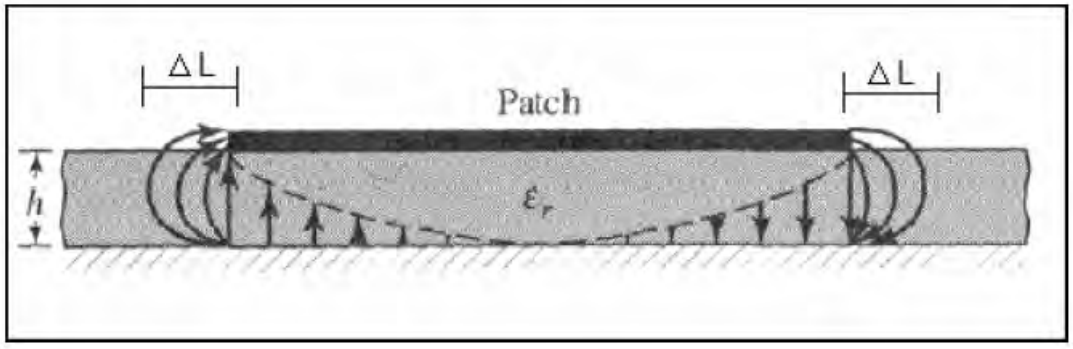

Figure 2.8: Fringing field effect in MSA.

When $\frac{w}{h} > 1$ the ε_{reff} *of the MSA could be found using [1]*

$$_{reff} = \frac{_1 + 1}{2} + \frac{_r - 1}{2}\left[1 + 12\frac{h}{w}\right]^{-1/2} \qquad (2.5)$$

Where $1 < \varepsilon_{reff} < \varepsilon_r$ *and* ε_{reff} *is a function of frequency (2.6), so when frequency of operation increases, most of the electric field lines concentrate in the substrate.*

We can find the effective length using the following equations [1].

$$L_{eff} = \frac{c}{2 f_0 \sqrt{_{reff}}} \qquad (2.6)$$

To find the length extension, we use the following equation

$$\Delta L = 0.412h\left(\frac{\left(\varepsilon_{reff}+0.3\right)\left(\frac{w}{h}+0.264\right)}{\left(\varepsilon_{reff}-0.258\right)\left(\frac{w}{h}\right)+0.8}\right) \qquad (2.7)$$

The actual length of the patch

$$L_{eff} = L + \Delta L \qquad (2.8)$$

For practical considerations, it is essential to have a finite ground plane, but this is critical issue where by, if the ground plane width goes below a certain value, relatively very sharp variation in the impedance bandwidth would occur [13]. To calculate the ground plane dimensions (L_{ground}, W_{ground}), it has been shown that similar results for finite and infinite ground plane can be obtained if the size of the ground plane is greater than the patch dimensions by approximately six times the substrate thickness all around the periphery. Hence, for this design, the ground plane dimensions would be given as:

$$L_{ground} = 6h + L$$

$$W_{ground} = 6h + W \qquad (2.9)$$

It is not practical to have *ground W less* than 30 mm. This is because ground plane width affects the radiation pattern, resonant frequency, radiation conductance, and gain by the diffraction of radiation from the edges of the ground plane. However, increasing the width of the ground plane, the impedance bandwidth and the resonant frequency will increase. The aperture conductance G_L and the resonant input impedance are given by [1].

$$G_1 = \frac{1}{120^{\ 2}} \int \left[\frac{\sin\left(\frac{k_0 w}{2} \cos \right)}{\cos} \right]^2 \sin^3 \ d \qquad (2.10)$$

$$R_{in} = \frac{1}{2G_1}$$

where $k_0 = \sqrt{\ }$ is the wave number. If we take the mutual effects between the slots into account, equation (2.10) is modified to

$$R_{in} = \frac{1}{2(G_1 \pm G_{12})} \qquad (2.11)$$

The mutual conductance G_{12} is found as follows [1]

$$G_{12} = \frac{1}{120^{\ 2}} \int_0 \left[\frac{\sin \frac{k_0 w}{2} \cos}{\cos} \right]^2 J_0(K_0 L \sin \ ) \sin^3 \ d \qquad (2.12)$$

where J_0 is the Bessel function of the first kind of order zero.
The (+) sign in equation (2.11) is used for modes with odd resonant voltage distributions beneath the patch and between the slots while (-) sign is used for modes with even resonant voltage distributions. Since

the desired place to fix the coaxial cable with the patch is where the impedance is 50 Ω, then we have to find the distance (x_0) between the feeding point and the leading radiating edge. This can be accomplished using [5]

$$R_{in}(x=x_0)=R_{in}(x=x_0)\cos^2\left(\frac{-}{L}x_0\right) \qquad (2.13)$$

2.4.2. Cavity Model

In order to gain insight into the radiating mechanism of a microstrip antenna, we need to first understand the near-field quantities that are present on the structure. The cavity model aids in this pursuit since it provides a mathematical solution for the electric and magnetic fields of a microstrip antenna. It does so by using a dielectrically loaded cavity to represent the antenna. As we can see in Figure 2-9, this technique models the substrate material, but it assumes that the material is truncated at the edges of the patch. The patch and ground plane are represented with perfect electric conductors and the edges of the substrate are modeled with perfectly conducting magnetic walls. It should be noted that the cavity model does not include feed effects; the feed is shown in the figure simply for reference.0

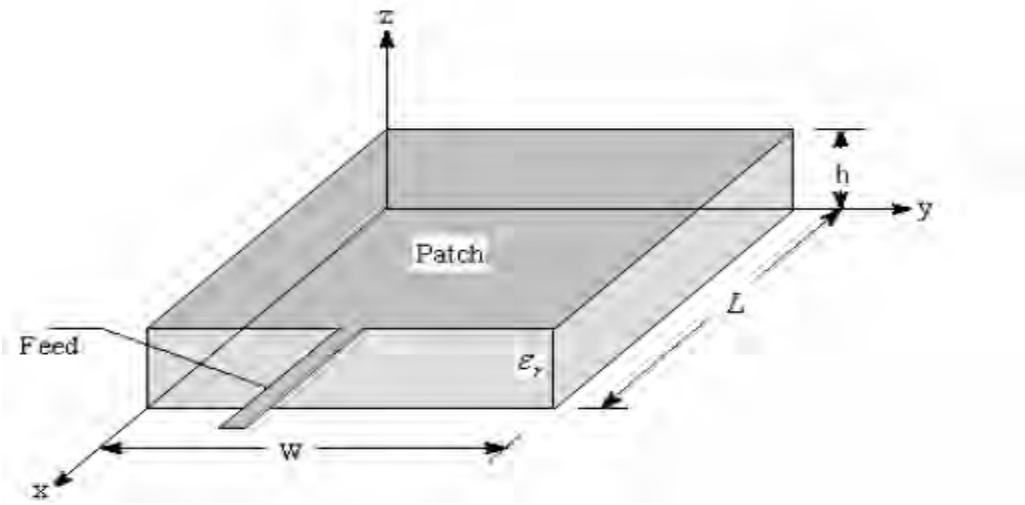

Figure 2.9 Geometry of cavity model for MSA.

Balanis formulates a solution to the above cavity problem using the vector potential approach [2] and [1]. Summarizing the technique, we begin by assuming that the dielectric is very thin, which means that the electric field is constant along the height of the substrate, h, and is nearly normal to the surface of the patch. Therefore, we only need to consider *z TM* modes inside the cavity. Now, we can write an expression for the electric and magnetic fields within the cavity in terms of the vector potential A_z [2]:

$$\boldsymbol{E}_x = -\boldsymbol{j}\frac{1}{\boldsymbol{\omega\varepsilon}}\frac{\partial^2 \boldsymbol{A}_z}{\partial \boldsymbol{x}\partial \boldsymbol{y}} \qquad \boldsymbol{H}_x = \frac{1}{\boldsymbol{\mu}}\frac{\partial \boldsymbol{A}_z}{\partial \boldsymbol{y}}$$

$$\boldsymbol{E}_y = -\boldsymbol{j}\frac{1}{\boldsymbol{\omega\varepsilon}}\frac{\partial^2 \boldsymbol{A}_z}{\partial \boldsymbol{y}\partial \boldsymbol{z}} \qquad \boldsymbol{H}_Y = \frac{1}{\boldsymbol{\mu}}\frac{\partial \boldsymbol{A}_z}{\partial \boldsymbol{x}} \qquad (2.14)$$

$$\boldsymbol{E}_Z = -\boldsymbol{j}\frac{1}{\boldsymbol{\omega\varepsilon}}\left(\frac{\partial^2}{\partial \boldsymbol{z}^2} + \boldsymbol{k}^2\right)\boldsymbol{A}_Z \qquad \boldsymbol{H}_Z = 0$$

Since the vector potential must satisfy the homogeneous wave equation

$$\nabla^2 \boldsymbol{A}_z + \boldsymbol{K}^2 \boldsymbol{A}_z = 0 \qquad (2.15)$$

We can use separation of variables to write the following general solution [10]

$$\boldsymbol{A}_z = [\boldsymbol{A}_1 \cos(\boldsymbol{k}_x \boldsymbol{x}) + \boldsymbol{B}_1 \sin(\boldsymbol{k}_x \boldsymbol{x})][\boldsymbol{A}_2 \cos(\boldsymbol{k}_y \boldsymbol{y}) + \boldsymbol{B}_2 \sin(\boldsymbol{k}_y \boldsymbol{y})][\boldsymbol{A}_3 \cos(\boldsymbol{k}_z \boldsymbol{z}) + \boldsymbol{B}_3 \sin(\boldsymbol{k}_z \boldsymbol{z})] \qquad (2.16)$$

Where K_x ,K_y and K_z are wave numbers. Applying boundary conditions

E_x=0 for 0≤x≤L,0≤y≤W,z=0

and 0≤x≤L, 0≤y≤W,z=h

H_x=0 for 0≤x≤L,y=0,0≤z≤h

and 0≤x≤L, y=w,0≤z≤h

H_Y=0 for x=L,0≤y≤W,0≤Z≤h

and x=L, 0≤y≤W,0≤Z≤h

We obtain a solution for the electric and magnetic fields inside the cavity as below [13]:

$$\boldsymbol{E}_x = -\boldsymbol{j}\frac{\boldsymbol{k}_x \boldsymbol{k}_z}{} \boldsymbol{A}_{mnp} \sin(\boldsymbol{k}_x \boldsymbol{x}) \cos(\boldsymbol{k}_y \boldsymbol{y}) \sin(\boldsymbol{k}_z \boldsymbol{z})$$

$$\boldsymbol{E}_y = -\boldsymbol{j}\frac{\boldsymbol{k}_y \boldsymbol{k}_z}{} \boldsymbol{A}_{mnp} \cos(\boldsymbol{k}_x \boldsymbol{x}) \sin(\boldsymbol{k}_y \boldsymbol{y}) \sin(\boldsymbol{k}_z \boldsymbol{z})$$

$$\boldsymbol{E}_z = -\boldsymbol{j}\frac{\boldsymbol{k}^2 - \boldsymbol{k}_z^{\,2}}{} \boldsymbol{A}_{mnp} \cos(\boldsymbol{k}_x \boldsymbol{x}) \cos(\boldsymbol{k}_y \boldsymbol{y}) \cos(\boldsymbol{kzz}) \qquad (2.17)$$

$$\boldsymbol{H}_x = -\frac{\boldsymbol{k}_y}{} \boldsymbol{A}_{mn\,p} \cos(\boldsymbol{k}_x \boldsymbol{x}) \sin(\boldsymbol{k}_y \boldsymbol{y}) \cos(\boldsymbol{k}_z \boldsymbol{z})$$

$$\boldsymbol{H}_y = -\frac{\boldsymbol{k}_x}{} \boldsymbol{A}_{mnp} \sin(\boldsymbol{k}_x \boldsymbol{x}) \cos(\boldsymbol{k}_y \boldsymbol{y}) \cos(\boldsymbol{k}_z \boldsymbol{z})$$

H_z=0

Where,

$$K_x = \frac{m}{L}, m = 0,1,2.....$$
$$K_y = \frac{n}{W}, n = 0,1,2..... \quad m = n = p \neq 0 \qquad (2.18)$$
$$K_z = \frac{p}{h}, p = 0,1,2...$$

and A_{mnp} is the amplitude coefficient. Finally, the resonance frequencies for the cavity are given by

$$(f_r)_{mnp} = \frac{1}{2\sqrt{\quad}}\sqrt{\left(\frac{m}{L}\right)^2 + \left(\frac{n}{W}\right)^2 + \left(\frac{p}{h}\right)^2} \qquad (2.19)$$

Examining the above fields for $(TM_z)_{100}$ dominant mode excitation, we see that $K_Y = K_Z = 0$ and the field components reduce to

$$E_z = -j\ A_{100}\cos\left(\frac{}{L}x\right)$$
$$H_y = \frac{}{L}A_{100}\sin\left(\frac{}{L}x\right) \qquad (2.20)$$

We can convert to equivalent electric and magnetic current densities using:

$$\vec{J} = nX\vec{H} \qquad (2.21)$$
$$\vec{M} = -nX\vec{E}$$

Where $n\hat{}$ is the outward directed surface normal. The magnetic field is zero along the $X = 0$ and $X = L$ walls and is normal to the surface along the $y = 0$ and $y = W$ walls. Therefore, no equivalent electric current density flows on the walls of the cavity. The electric field results in a non-zero magnetic current density on the walls of the cavity. Figure 2.10 shows both the electric field and corresponding

magnetic current densities for the microstrip antenna. The magnetic currents can be broken into a pair of radiating slots and a pair of non-radiating slots. The radiating slots are in phase so they will constructively interfere in the far-field. Thus, these two slots form the primary radiating mechanism for the microstrip antenna. On the other hand, the non-radiating slots are out of phase so they will destructively interfere in the far-field and will not contribute to the radiated fields.

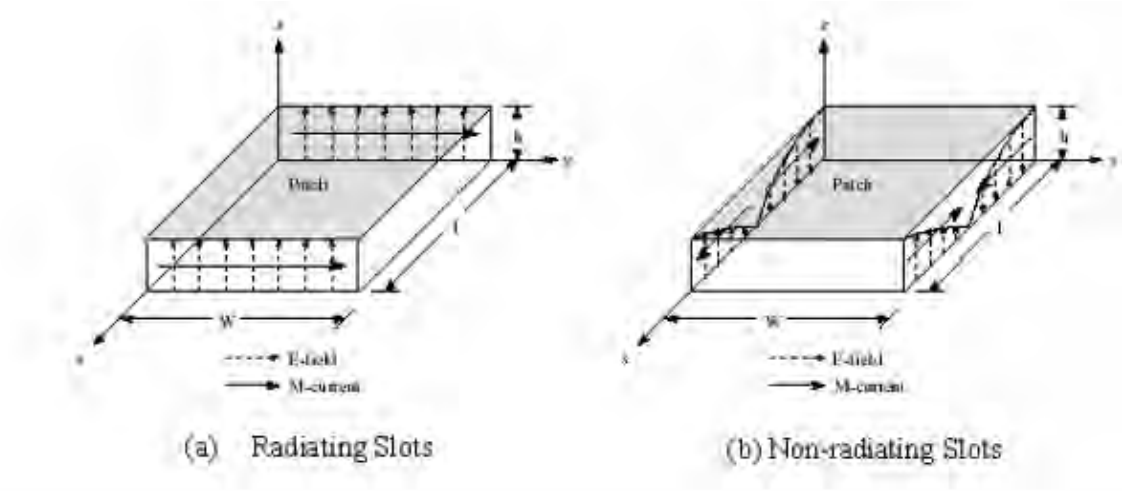

Figure 2.10 Field configurations and current densities for microstrip patch [1]

From the above results, we can see that the cavity model provides excellent insight into the radiating mechanism of a microstrip patch antenna. It provides the field configurations of the radiating and non-radiating slots that can be used to solve for the radiation patterns [1]. Since the antenna is modeled as a cavity, additional work is necessary to accurately model the input impedance. An effective loss tangent needs to be added to account for the power that is lost to radiation [1]. Alternatively, the radiated energy can be modeled using an impedance

boundary condition at the walls [9].Although the cavity model is quite adept at modeling the radiating mechanism for a microstrip antenna, it does have some limitations. First, the cavity model does not model the feed effects. Or does it model the adverse effects introduced by a finite substrate and ground plane. One way to circumvent these limitations is to employ numerical techniques.

2.4.3 Full-Wave Solutions – Method of Moments

In some instances, we may need to understand how the behavior of an antenna is affected by its surroundings. For example, we may want to develop a model that includes the effects of a feed structure, a finite ground plane, or a case enclosure. For problems such as these, the techniques described above become highly impractical.

Fortunately, there are a variety of numerical analysis techniques that can handle these problems quite nicely, including the method of moments (MoM), the finite-element method (FEM), and the FDTD method. All three of these techniques are computationally intensive, which in the past limited the size and complexity of problems that could be approached. However, due to recent advances in computing capabilities, these techniques have become much more powerful. In addition, these techniques are somewhat generalized so they are capable of modeling a variety of antennas (not just the microstrip patch). The details of each technique are quite intricate, so we will focus on the FDTD method because it is used to generate the examples presented in this thesis. The FDTD method uses a discretization in time and space to calculate a solution of Maxwell's curl equations directly in the time domain [13]:

i.e

$$\nabla X \vec{E} = - \frac{\partial \vec{H}}{\partial t}$$
$$\nabla X \vec{H} = \frac{\partial \vec{E}}{\partial t} + \vec{J} \qquad (2.22)$$

Rearranging these equations

$$\frac{\partial \vec{H}}{\partial t} = -\frac{1}{-} \nabla X \vec{E}$$
$$\frac{\partial \vec{E}}{\partial t} = \frac{1}{-} \nabla X \vec{H} - \frac{\Delta}{-} \vec{E} \qquad (2.23)$$

Evaluating the vector curl operator (∇XA) and employing central differencing in both time and space to approximate the partial derivatives, we obtain six updated equations (one for each component of the electric and magnetic fields). For example, the updated equation for the E_x component is as follows

$$E_x^n(i,j,k) = \left[\frac{}{+\Delta} \right] E_x^{n-1}(i,j,k) + \left[\frac{\Delta t}{+\Delta} \right] \left[\frac{H_z^{n-1/2}(i,j,k) - H_z^{n-1/2}(i,j-1,k)}{\Delta y} - \frac{H_y^{n-1/2}(i,j,k) - H_y^{n-1/2}(i,j,k-1)}{\Delta z} \right]$$

(2.24)

The electromagnetic structure is modeled by approximating its geometry and composition with Yee cells of different material parameters (both conductivity and relative dielectric constant). Figure 2-11 depicts an example Yee cell along with its corresponding field calculation points[11].

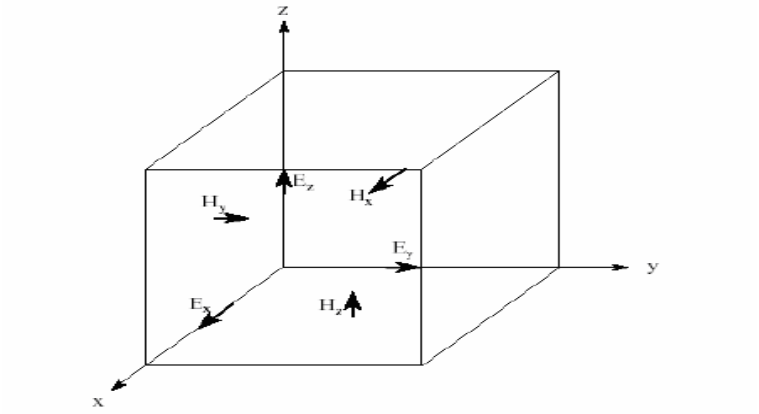

Figure 2-11 Example Yee cell with field calculation points

At the outer boundaries of the computational space an absorbing boundary condition is used to simulate free-space radiation. In order to avoid numerical instabilities in the finite-difference algorithm, the time increment must not violate the Courant stability condition [11]:

$$\Delta t \leq \frac{(\quad)^{1/2}}{\left[\frac{1}{\Delta x^2}+\frac{1}{\Delta y^2}+\frac{1}{\Delta z^2}\right]^{1/2}} \qquad (2.25)$$

An excitation is then applied to the computational model and the E - and H –field computations are alternately marched through time from time zero to the desired stopping point. Results can be viewed either in the time domain or in the frequency domain. In order to obtain the

frequency characteristics of the antenna it is necessary to compute a fast-Fourier transform (FFT) of the transient output data.

The FDTD techniques presented above allow antennas to be modeled in fine detail. Feed lines, finite ground planes, and case enclosures can all be included in the computational model. In addition, the techniques are highly generalized so a number of antennas can be analyzed. Tirkas and Balanis [14] demonstrate the versatility of FDTD techniques by using it to model a dipole, open-ended waveguide, and horn antenna. The major drawback of numerical techniques in general is that they generate huge amounts of data. However, we can alleviate this problem greatly through the use of visualization[1].

2.5 Performance Parameters of Microstrip Patch Antennas

2.5.1 Introduction

The purpose of a transmitting antenna is to radiate electromagnetic waves into "free space" (usually, but not necessarily, air). The power for this is supplied by a “feeder” (usually the feeder conveys power from a transmitter at some distance from the radiating structure, or from the antenna in receive mode to a receiver also at some distance from the structure) which is often a length of transmission line or wave guide having a well-defined characteristic impedance.

Antennas are also used in "receive mode" to collect radiation from "free space" and deliver the energy contained in the propagating wave to the feeder and receiver. Usually, antennas are reciprocal devices; their essential properties do not depend on whether they are used as transmit or receive devices. So an efficient transmit antenna can also be used as an efficient receive antenna for the same kind of signal. The directional pattern also does not depend on the transmit or receive mode usage. These properties are collected together and called reciprocity. What is the basic principle for the antenna to radiate?

A conducting wire radiates mainly because of time-varying current or acceleration (or deceleration) of charge. If there is no motion of charges in a wire, no radiation takes place, since no flow of current occurs. Radiation will not occur even if charges are moving with uniform velocity along a straight wire. However, charges moving with uniform velocity along a curved or bent wire will produce radiation. If the charge is oscillating with time, then radiation occurs even along a straight wire [1].

The radiation from an antenna can be explained with the help of Figure 2.12, which shows a voltage source connected to a two conductor transmission line. When a sinusoidal voltage is applied across the transmission line, an electric field is created which is sinusoidal in nature and these results in the creation of electric lines of force which are tangential to the electric field. The magnitude of the electric field is indicated by the bunching of the electric lines of force. The free electrons on the conductors are forcibly displaced by the electric lines of force and the movement of these charges causes the flow of current which in turn leads to the creation of a magnetic field.

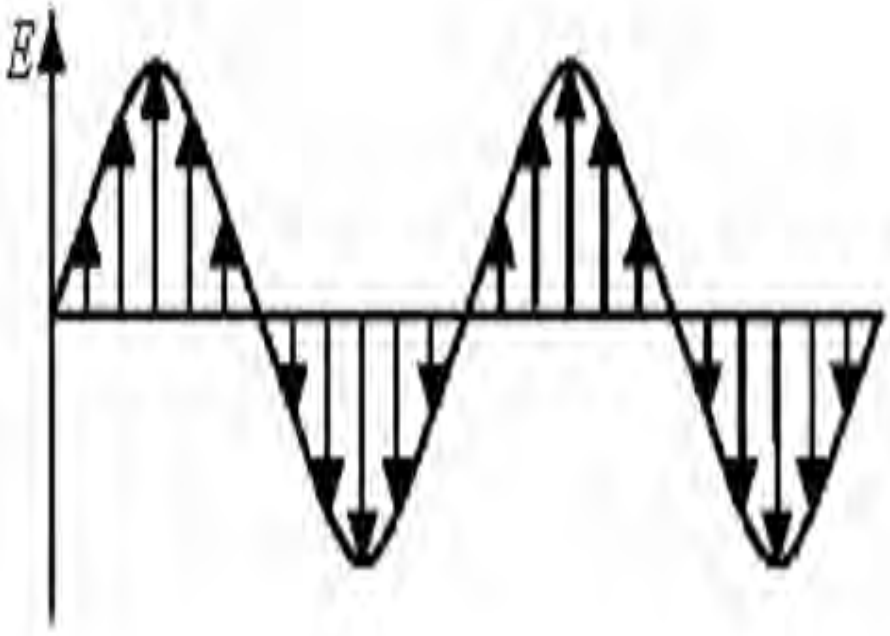

(a)

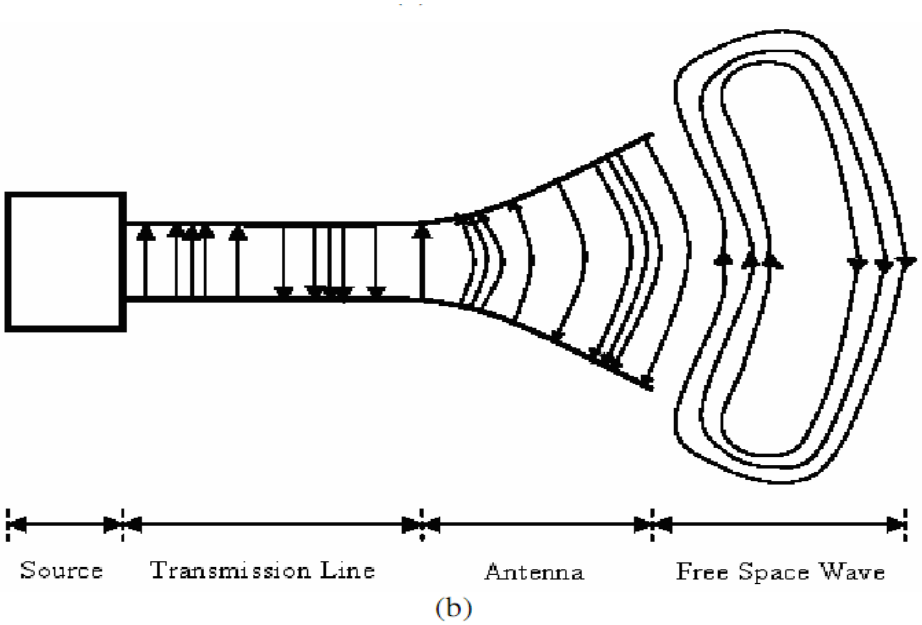

Fig 2.12: Radiation from antenna

Due to the time varying electric and magnetic fields, electromagnetic waves are created and these travel between the conductors. As these waves approach open space, free space waves are formed by connecting the open ends of the electric lines. Since the sinusoidal source continuously creates the electric disturbance, electromagnetic waves are created continuously and these travel through the transmission line, through the antenna and are radiated into the free space. Inside the transmission line and the antenna, the electromagnetic waves are sustained due to the charges, but as soon as they enter the free space, they form closed loops and are radiated [1].

The field patterns, associated with an antenna, change with distance and are associated with two types of energy: - radiating energy and reactive energy. Hence, the space surrounding an antenna can be divided into three regions. These are:

(a) Reactive near-field region: In this region, the reactive field dominates. The reactive energy oscillates towards and away from the antenna, thus appearing as reactance. In this region, energy is only stored and no energy is dissipated. The outermost boundary for this region is at a distance $R_1=062\sqrt{\boldsymbol{D}^3}$ where R, is the distance from the antenna surface, D is the largest dimension of the antenna and is the wavelength.

(b) Radiating near-field region (also called Fresnel region): This is the region which lies between the reactive near-field region and the far field region. Reactive fields are smaller in this field as compared to the reactive near-field region and the radiation fields dominate. In this region, the angular field distribution is a function of the distance from the antenna. The outermost boundary for this region is at a distance $R_2= 2\boldsymbol{D}^2 \diagup$ where R_2 is the distance from the antenna surface.

(c) Far-field region (also called Fraunhofer region): The region beyond the far field region. In this region, the reactive fields are absent and only the radiation fields exist. The angular field distribution is not dependent on the distance from the antenna in this region and the power density varies as the inverse square of the radial distance in this region. The performance of an antenna is measured in effectively transmitting or receiving the radiation fields.

2.5.2 Radiation Pattern

The radiation pattern of an antenna is usually described as directivity (in dB) of the antenna at different far field points as a function of spatial spherical coordinates (θ, φ). The far field radiation pattern of a typical half wavelength rectangular patch antenna on the ground plane has the maximum radiation occurs at the direction perpendicular to the patch surface (zenith where $\theta = 0^0$), and theoretically zero radiation along the surface of the patch (horizontal where $\theta = 90^0$). The patch antenna radiates into the upper half of the space and has no back lobe radiation if the ground plane is infinitely large. In real applications, a finite ground plane is used, thus there will be radiation over the whole space and the amount of the back lobe radiation will be a function of the ground plane size.

2.5.3 Reflection Coefficient (Γ) and Characteristic Impedance (Z_0)

When considering higher frequency applications, a prominent phenomenon that must be taken into account is the idea of reflection that occurs in microwave transmission lines. Every transmission line has a resistance associated with it, and comes about because of its construction. This is called its characteristic impedance, Z_0. The standard characteristic impedance value is 50Ω. However when the transmission line is terminated with an arbitrary load Z_L, in which is not equivalent to its characteristic impedance ($Z_L \neq Z_0$), a reflected wave will occur.

A reflection coefficient, Γ, is defined to give a measure of this phenomenon. It is derived by normalizing the amplitude of the reflected voltage V_0^-, to the amplitude of the incident wave, V_0^+, and is given as:

$$\Gamma = \frac{V_o^-}{V_o^+} = \frac{Z_L - Z_o}{Z_L + Z_o} \qquad (2.26)$$

2.5.4 Return Loss (RL)

The Return Loss is a parameter that indicates the amount of power that is lost to the load and does not return as a reflection. When the transmitter and antenna impedance do not match, waves are reflected leading to the formation of standing waves. Hence the RL is a parameter similar to the VSWR to indicate how well the matching between the transmitter and antenna has taken place. The RL is given by :

$$\mathrm{RL} = -20\log|\Gamma| \ \ (dB) \qquad (2.27)$$

For perfect matching between the transmitter and the antenna, Γ = 0 and RL = ∞ which means no power would be reflected back, whereas a Γ = 1 has a RL = 0dB, which implies that all incident power is reflected. For practical applications, a VSWR of 2 is acceptable, since this corresponds to a return loss of -9.54 dB.

2.5.5 Polarization

The term polarization has several meanings. In a strict sense, it is the orientation of the electric field vector E at some point in space. If the E-field vector retains its orientation at each point in space, then the polarization is linear; if it rotates as the wave travels in space, then the polarization is circular or elliptical. In most cases, the radiated-wave polarization is linear and either vertical or horizontal. At sufficiently large distance from an antenna, beyond 10 wavelengths, the radiated, far-field wave is a plane wave.

2.5.6 Directivity, Gain, and Radiation Efficiency

Directivity *D* of an antenna is the measure of energy concentrated in the main beam, which is equal to the ratio of radiation intensity in a given direction compared to an isotropic antenna. A simple estimate for the directivity of a rectangular patch is given by [2]:

$$D = \frac{4(k_0 W)^2}{\pi \eta_0 Y_{in}} \qquad (2.28)$$

Where k_0, is wave number

W, is width of patch

Y_{in}, is input admittance

η_0, is characteristic impedance

The directivity is always greater than one since an isotropic antenna is non-directional. The gain *G* is slightly less than directivity and takes into consideration any losses associated with the antenna. Gain *G* is related to directivity *D* by radiation efficiency:

$$G = e_r \cdot D \qquad (2.29)$$

The radiation efficiency is the ratio of the radiated power to the input power and accounts for conduction, dielectric, and surface wave losses associated with the structure. Radiation efficiency can be expressed as

$$e_r = \frac{P_r}{P_r + P_c + P_d + P_{sur}} \qquad (2.30)$$

Where p_r, is radiated power

P_{sur}, is surface wave power

$P_{d,}$ is dielectric power loss

$P_{c,}$ conduction power loss

For a low loss substrate powers associated to conduction loss P_c and dielectric loss P_d are negligible. Radiated and surface wave powers can be obtained from the following equations respectively.

2.5.7 Voltage Standing Wave Ratio (VSWR)

In order for the antenna to operate efficiently, maximum transfer of power must take place between the transmitter and the antenna. Maximum power transfer can take place only when the impedance of the antenna (Z in) is matched to that of the transmitter (Zs).

If the condition for matching is not satisfied, then some of the power maybe reflected back and this leads to the creation of standing waves, which can be characterized by a parameter called as the Voltage Standing Wave Ratio (VSWR). The VSWR can be expressed as

$$SWR = \frac{V_{max}}{V_{min}} = \frac{1 + |\Gamma|}{1 - |\Gamma|} = \frac{1 + S_{11}}{1 - S_{11}} \qquad (2.31)$$

The VSWR expresses the degree of match between the transmission line and the antenna. When the VSWR is 1 to 1 (1:1) the match is perfect and all the energy is transferred to the antenna prior to be radiated. In an antenna system, its reflection coefficient is also its $S_{11.}$ In addition, for an antenna to be reasonably functional, a minimum VSWR≤1.5 is required.

2.5.8 Bandwidth

The bandwidth of an antenna is defined by "the range of usable frequencies within which the performance of the antenna, with respect to some characteristic, conforms to a specified standard." The bandwidth can be the range of frequencies on either side of the center frequency where the antenna characteristics like input impedance, radiation pattern, beam width, polarization, side lobe level or gain, are close to those values which have been obtained at the center frequency.

The bandwidth of a broadband antenna can be defined as the ratio of the upper to lower frequencies of acceptable operation. The bandwidth of a narrowband antenna can be defined as the percentage of the frequency difference over the center frequency. According to these definitions can be written in terms of equations as follows:

$$BW_{broadband} = \frac{f_H}{f_L} = 2$$

$$BW_{narrowband}(\%) = \left[\frac{f_H - f_L}{\sqrt{f_H \times f_L}}\right] \times 100 \qquad (2.32)$$

Where, f_H is upper frequency

f_L is lower frequency

An antenna is said to be broadband if $\frac{f_H}{f_L} = 2$. One method of judging how efficiently an antenna is operating over the required range of frequencies is by measuring its VSWR. A VSWR≤ 2 (RL≥ -9.5dB) ensures good performance.

2.6 Bandwidth Improvement Techniques for Microstrip Antenna

As a technique to increase the impedance bandwidth, two techniques, stacked patches and coplanar parasitic patches are proposed.

2.6.1 Stacked patches configuration

As a technique or the purpose of broad banding (to increase the impedance bandwidth), two or more patches on different layer of the dielectric substrates are stacked on each other. This kind of configuration is categorized as electro-magnetically coupled microstrip antenna.

The basic configuration of electro magnetically coupled microstrip antenna is shown below.

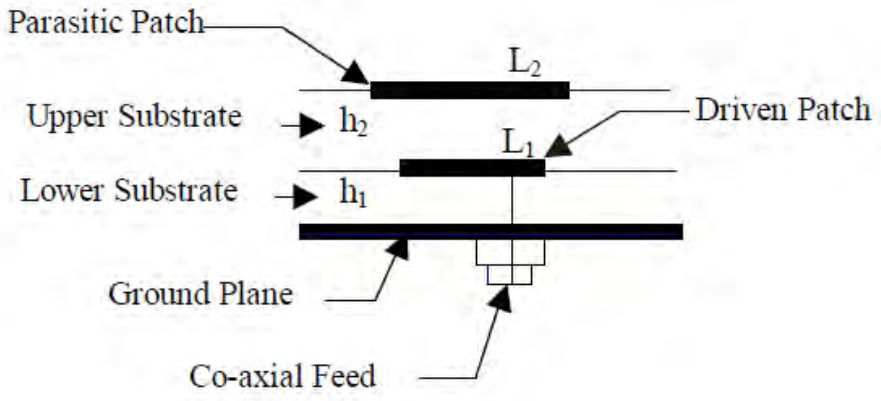

fig.2.13: Multi layer electro-magnetically coupled stacked patch Microstrip antenna

The bottom patch is fed with a coaxial line, and the top parasitic patch is excited due to the electromagnetic coupling with the bottom

patch. The patches can be fabricated on different substrates, and air gap or foam material can be placed between these layers to create height thus increasing the bandwidth. Here, the patch dimensions are optimized so that the resonance frequencies of the two patches are close to each other to yield a broad bandwidth. It was studied that the electromagnetically coupled microstrip antenna with two or three layers of patches provides an improved impedance bandwidth for VSWR ≤ 2.

2.6.2 Coplanar Parasitic Configurations

Coplanar parasitic elements can be coupled either to the radiating or non-radiating edges of the driven patch or both. Typically coplanar parasitic elements have been separated from the driven element by a narrow gap, but to increase the coupling, they can also have a direct (galvanic) contact to it. In addition to increasing bandwidth, a major advantage of the coplanar configuration is easy fabrication because only one dielectric layer is required. Increased surface area and antenna size are often stated as disadvantages of coplanar parasitic

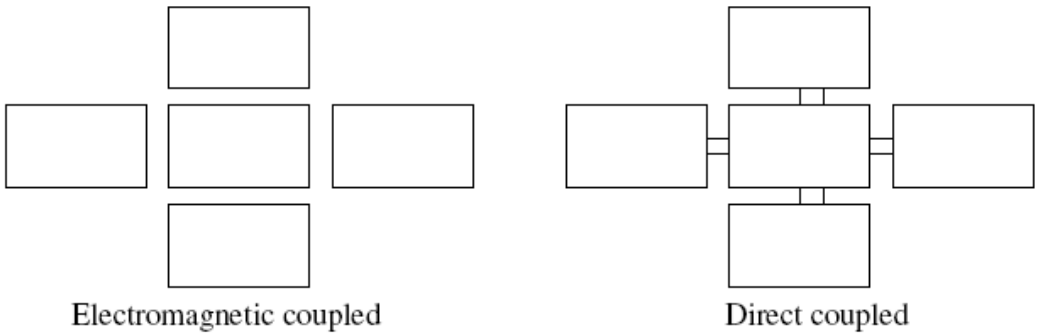

Fig.2.14 coplanar Parasitic Configurations

CHAPTER3

DESIGN OF CONVENTIONAL AND STACKED MICROSTRIP ANTENNA.

3.1 Design of a Conventional Microstrip Antenna

This chapter explains in detail the procedure of designing a square microstrip patch antenna. A conventional square patch is designed as a reference and another stacked configuration method will be used to design the square microstrip patch antenna with enhanced bandwidth and gain.

The main factors involved in the design of a single patch antenna are:

_ Selection of substrate material

_ Feed position & its location

_ Patch dimensions

For the selection of substrate, the major electrical properties to consider are relative dielectric constant. The selection of substrate material plays a very important role in patch antenna design. A higher dielectric constant results in smaller patch but generally reduces bandwidth resulting in tighter fabrication tolerance. The substrate thickness should be chosen as large as possible to maximize bandwidth and efficiency, but not so large to risk surface wave excitation.

3.1.1 Design Specification

A square patch microstrip antenna is chosen because it simplifies the analysis and the performance prediction.

The three essential parameters for the design of a rectangular Microstrip Patch Antenna are:

_ Frequency of operation (f_o): The resonant frequency of the antenna must be selected appropriately. The wireless local area network (WLAN) for which the application of the MSA is desired, operates in the frequency range of 2.4_2.5 GHz. Hence the antenna designed must be able to operate in this frequency range. The resonant frequency selected in this case is 2.45 GHz.

_ Dielectric constant of the substrate ($_r$): The dielectric material selected in this thesis has a dielectric constant of 3.1

_ Height of dielectric substrate (h): For the microstrip patch antenna to be used in the aforementioned frequency range, the antenna size may be moderate in thickness. In this design, the height of the dielectric substrate is selected is 1.8mm.

3.1.2 Design Procedure

Step1. Calculation of the width (W): the width of the microstrip patch antenna is given by equation (2.4) as [1]:

$$W = \frac{c}{2f_r}\sqrt{\frac{2}{(\varepsilon_r+1)}} \qquad (2.4)$$

Substituting c=3x10^8 m/s ε_r=3.1 and f_o=2.45GHz.we get W=42.76mm

Step 2: Calculation of effective dielectric constant (ε_{reff}) :

$$_{reff} = \frac{_1+1}{2} + \frac{_r-1}{2}\left[1+12\frac{h}{w}\right]^{-1/2} \qquad (2.5)$$

Substituting, ε_r =3.1, W=42.76mm and h=1.8mm we get ε_{reff} =2.90575

Step 3: Calculation of the effective length (L_{eff}):

$$L_{eff} = \frac{c}{2 f_r \sqrt{\varepsilon_{eff}}} \qquad (2.6)$$

Substituting, ε_{reff} =2.90575 c=3x10^8 m/s and f_o=2.45GHz we get L_{eff} =35.91mm

Step 4: Calculation of the length extension (ΔL)

$$\Delta L = 0.412h \frac{(\varepsilon_{reff} + 0.3)\left(\frac{W}{h} + 0.264\right)}{(\varepsilon_{reff} - 0.258)\left(\frac{W}{h} + 0.8\right)} \qquad (2.7)$$

ΔL=0.854mm

Step 5: Calculation of the actual length of the patch (L):

$$L = L_{eff} - 2\Delta L$$

L=34mm

From the calculation, the width of the patch is 42.76mm and the patch length is 34mm. However, in this thesis the square patch is chosen because it simplifies analysis and performance prediction. The width and length chosen is 34 mm.

The area of conventional microstrip antenna is

34mmx34mm=1156$(mm)^2$

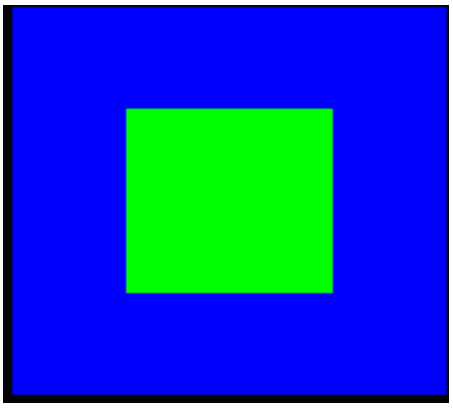

Fig.3.1 Geometry of conventional microstrip antenna

Step 6: Calculation of the ground plane dimensions (Lg and Wg)

The transmission line model is applicable to infinite ground planes only. However, for practical considerations, it is essential to have a finite ground plane. It has been shown in many open literatures [1][6][13] that similar results for finite and infinite ground planes can be obtained if the size of the ground plane is greater than the patch dimensions by approximately six times the substrate thickness all around the periphery. Hence, for this design, the ground plane dimensions would be given as:

$$L_g = 6h + L = 6 \text{ x}1.8 \text{ mm} + 34\text{mm} = 44.8\text{mm}$$

$$W_g = 6h + W = 6\text{x } 1.8 \text{ mm} + 34\text{mm} = 44.8\text{mm}$$

Calculation result of conventional patch microstrip antenna is given in Table 3.1

Design results of a conventional square microstrip antenna	
Width of patch, (W)	34mm
Length of patch , (L)	34mm
Effective dielectric constant, (ε_{eff})	2.90575
Height of substrate (h)	1.8mm
Feeding point,(x,y)	15.1mm,19.3mm

Table3. 1, calculated result of a conventional square microstrip antenna

3.2 Methods for Reducing the Size of Microstrip Antenna

Size miniaturization of microstrip patch antenna is increasingly essential in many practical applications, such as mobile cellular handsets, cordless phones, direct broadcast satellites (DBS), wireless local area networks (WLAN), global position satellites (GPS) and other next-generation wireless terminals.

Applications in present-day mobile communication systems usually require smaller antenna size in order to meet the miniaturization requirements of mobile units. Thus, size reduction is becoming major design considerations for practical applications of microstrip antennas. For this reason, studies to achieve compact microstrip antennas have greatly increased. Much significant progress in the

design of compact microstrip antennas has been reported over the past several years [1][13].

In general, the size miniaturization of the normal microstrip patch antenna has been accomplished by loading, which can take various forms, namely;

i. Use of high dielectric constant substrates
ii. Modification of the basic patch shapes;
iii. Use of short circuits, shorting-pins or
Shorting- posts; and
iv. A combination of the above techniques.

Employing high dielectric constant substrates is the simplest solution, but it exhibits narrow bandwidth, high loss and poor efficiency due to surface wave excitation.

Modification of the basic patch shapes allows substantial size reduction.

In this work, applying u- shape on four sides of square microstrip patch antenna a significant size reduction is obtained. However size reduction comes at the cost of bandwidth and gain which is then enhanced to a good level using stacked configuration on a reduced size microstrip patch antenna.

Geometry of the modified shape patch antenna

The reduced size microstrip patch antenna configuration is shown in Figure 3.2. The patch has dimensions of WXL=24mmx24mm. This has a reduced area compare to conventional patch antenna which has WXL=34mmx34mm.For further reduction, the modified shape patch

antenna uses four equal u-shape on all sides of a patch with length of 10mm and width of 6mm.

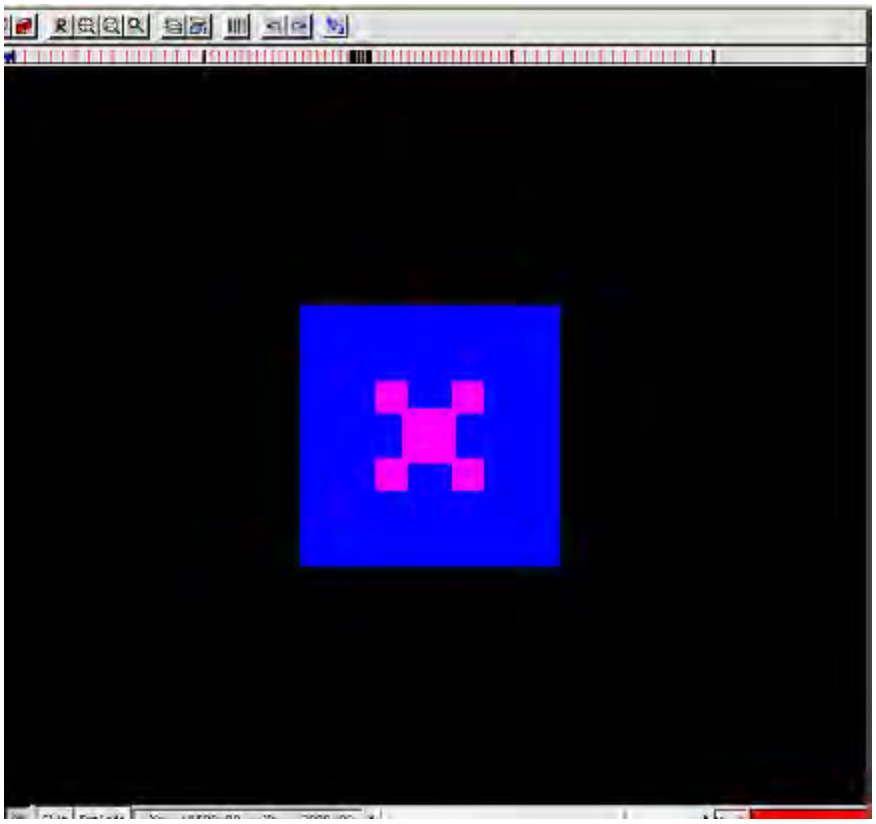

Fig.3.2 Geometry of the modified shape microstrip patch antenna

The area of the modified shape patch is given by

$$A_{modified} = A_{total} - 4A_{u\text{-}shape}$$

Where, $A_{total} = 24mm \times 24mm = 576\ mm^2$

$$A_{u\text{-}shape} = 10 \times 6 = 60\ mm^2$$

$$A_{modified} = 336\ mm^2$$

Comparing this area with conventional microstrip antenna which is $1156\ mm^2$, the area of proposed antenna is reduced by around 70%.

3.3 Stacked MSA Design

In this configuration two microstrip patches with equal sizes are stacked on top of each other on a common ground plane. The stacked layer structure is used for increasing bandwidth and gain of the antenna, in which the top patch layer is responsible for radiation and it is fed by coupling through the lower layer.

The modified shape patch antenna uses four equal size u-shape on each patch. Thus the effective size of the patch is reduced.

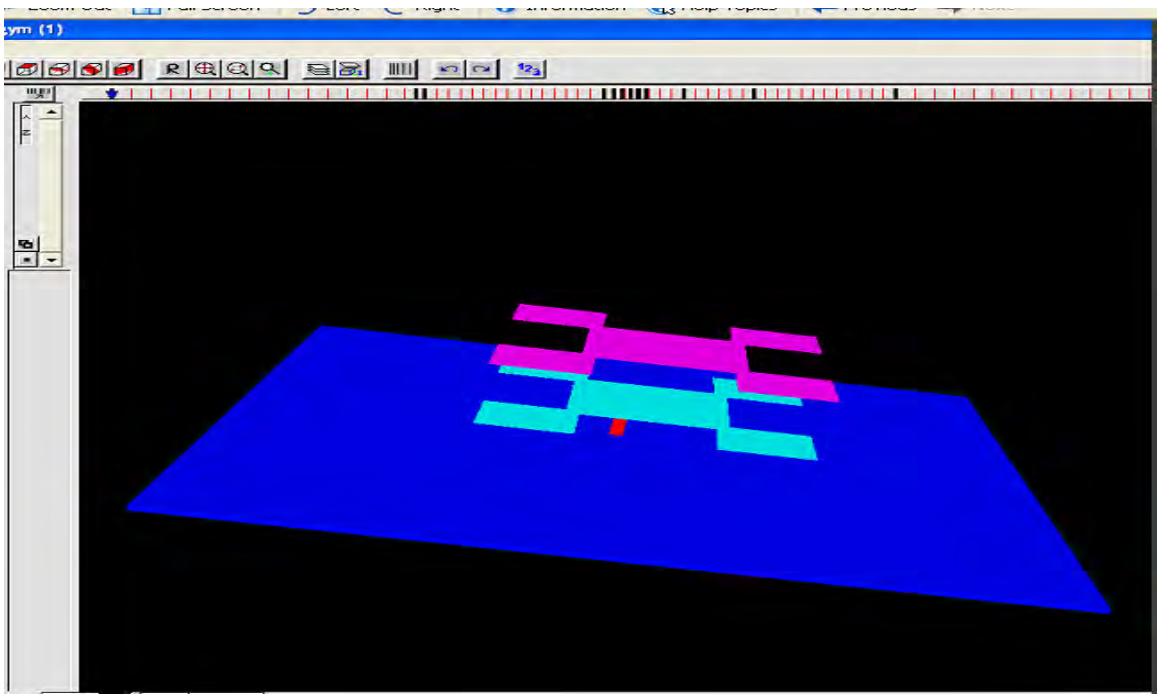

Fig 3.3 Geometry of modified shape stacked layer microstrip antenna

In the typical design procedure of the microstrip antenna, the first step is to select the dielectric substrate and then to fix the thickness h_1 and h_2. The dielectric constant selected for lower substrate is

3.1with thickness h_1 of 4.6 mm whereas the upper substrate is with dielectric constant of 1.6 and thickness h_2 of 7 mm. The u-shape dimensions of both the patches (driven and parasitic) are selected as optimization variable with objective to get the central frequency 2.45 GHz and to cover the whole operating range of WLAN. After much trial the dimensions selected for stacked configuration microstrip antenna which gives a better performance is summarized in the table below.

Results

Design results of a stacked configuration of microstrip antenna	
Width of lower patch,w_1	24mm
Length of lower patch, L_1	24mm
Height of lower patch ,H_1	4.6mm
Effective dielectric constant ε_{eff1}	2.90575
Feeding point,x,y	12.5mm,12.6mm
Width of upper patch,W_2	24mm
Length of upper patch, L_2	24mm
Height of upper patch ,H_2	7.2mm
Effective dielectric constant ε_{eff2}	1.6

Table3.2 selected dimensions for stacked configuration microstrip anteenna

CHAPTER 4

SIMULATION RESULTS

Simulation of the antenna was performed using Empire simulator to obtain computational results for the designed conventional and stacked mirostrip antennas. The simulation method is based upon the explicit solution of Maxwell's equations in FDTD.

Considering the calculated dimensions of conventional and stacked microstrip antennas of Tables3.1 and 3.2, the performance of the antennas are simulated. The result of the simulations is presented below.

4.1) Lumped port feed conventional microstrip antenna.

Lumped elements

At RF and low microwave frequencies, lumped elements (R,L,C) can be effectively used to accomplish matching. Lumped elements have the advantages of small size, low cost and wider bandwidth as compared to distributed circuits. These are especially suitable for monolithic MICs and for broadband hybrid MICs where real-estate requirements are prime importance [1],[13].

Physical structure

Here a square microstrip patch of dimensions 2.82cmx2.82cm with dielectric substrate $_r$=4.4 and height of h= 0.16cm is feed with lumped port.

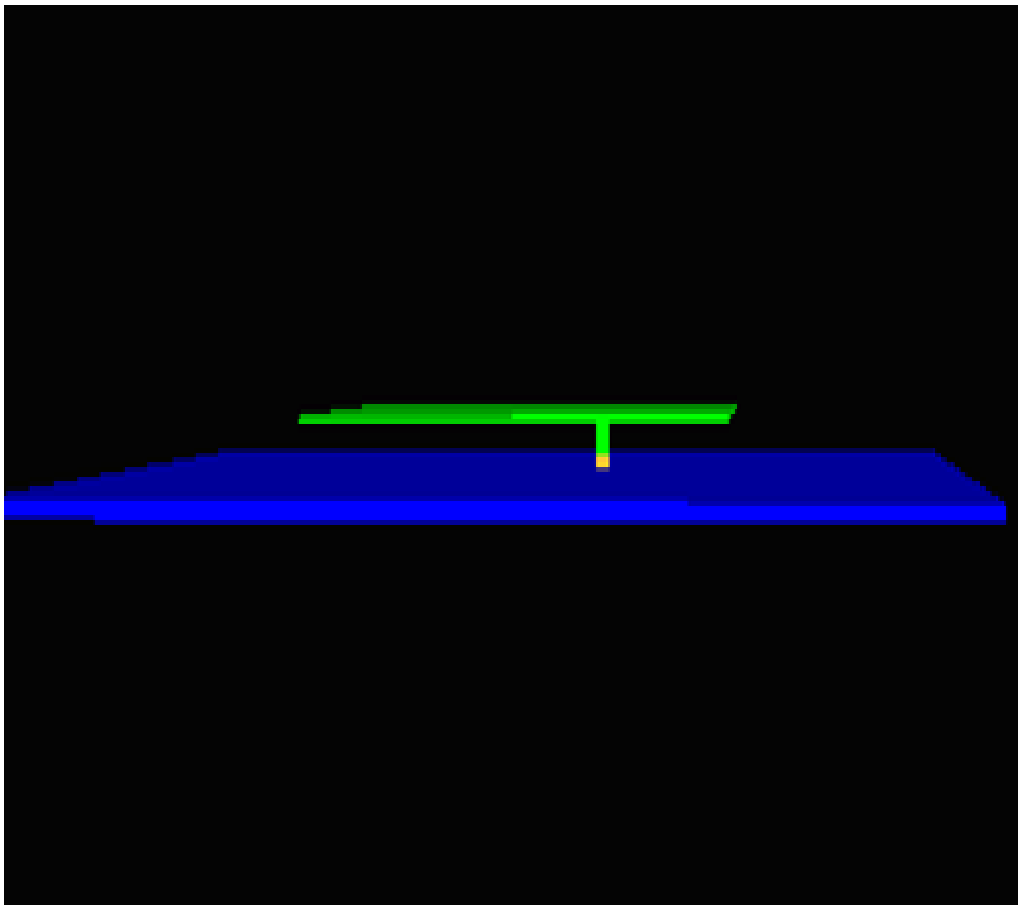

Fig 4.1 Physical structure of a conventional microstrip antenna

Results

A) Return Loss (S11 Parameter)

The simulated result of S11 scattering parameter of Conventional microstrip antenna is presented in Figure below. From the figure, the antenna has almost 2.45 GHz resonant frequency and it has 46.3MHz band width at 9.5 dB (the difference of 2.2.4418 GHz and 2.4878GHz).

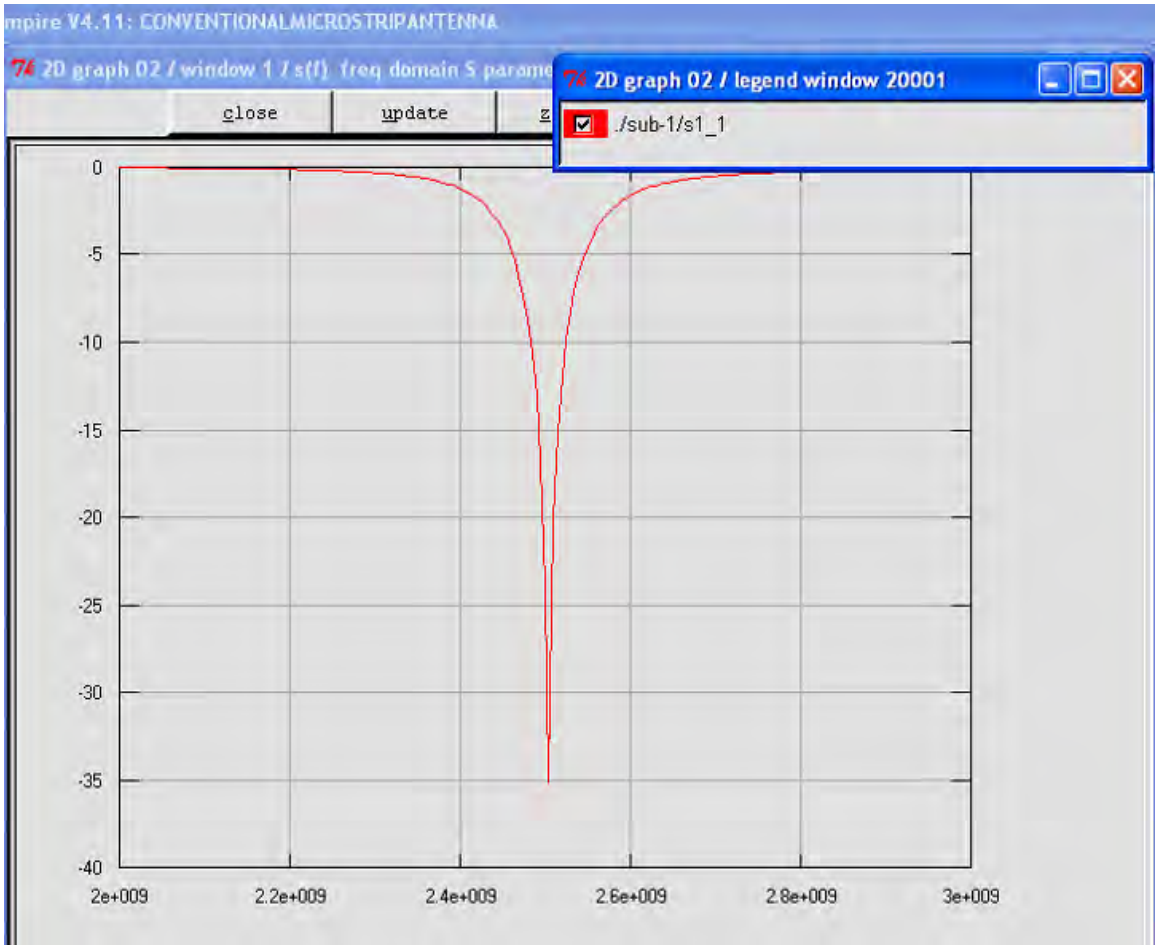

Fig 4.2 S11 of lumped port feed conventional MSA

B) The Smith chart plot

The Empire simulator also provides smith chart plot of lumped port feed conventional microstrip patch antenna. The result indicates that the line impedance magnitude of the patch antenna intersects the unit circle of the smith chart in the frequency range of 2.2.4418 GHz – 2.4878GHz . It crosses a unit circle, where the reflection coefficient| Γ | is zero, confirming no reflected power due to mismatching.

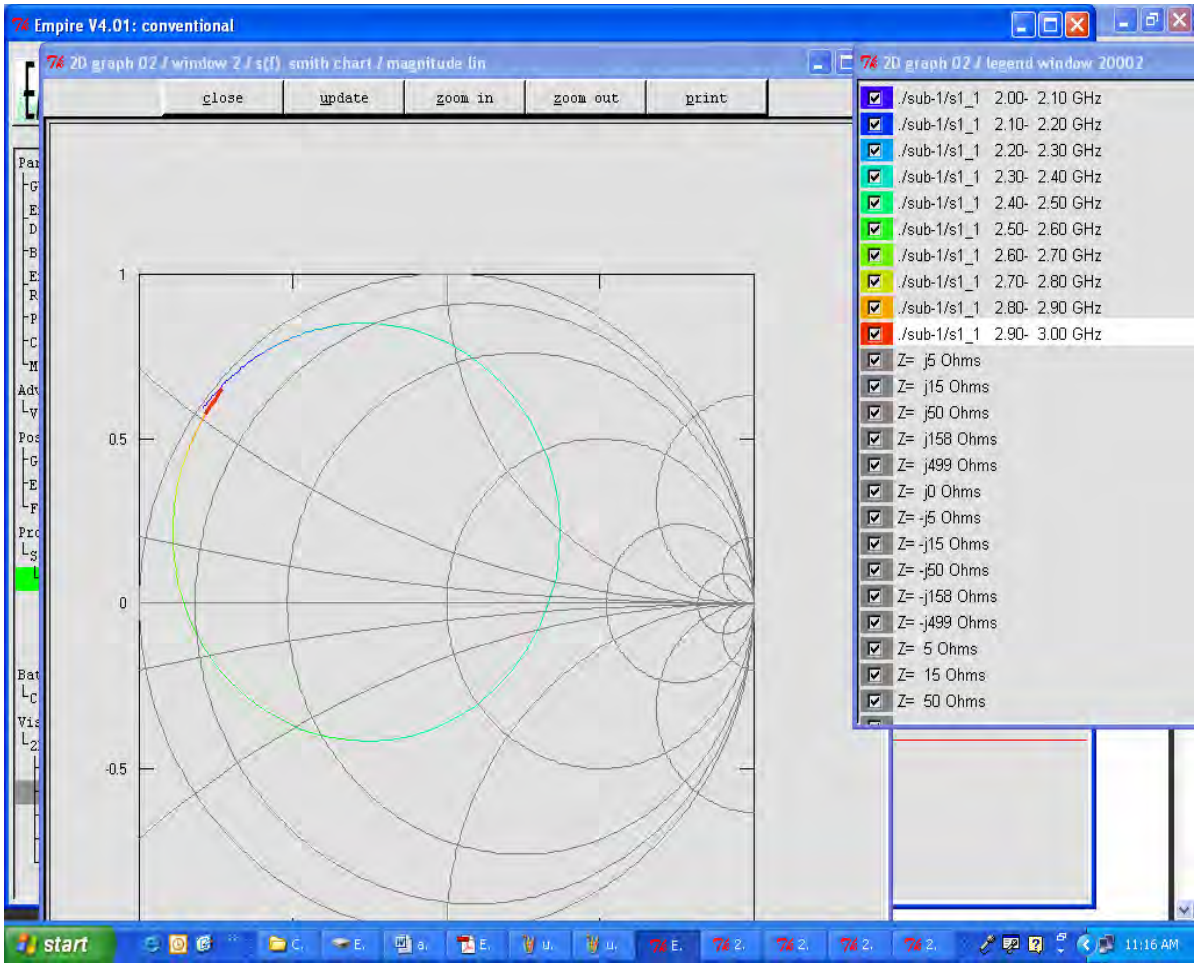

Fig 4.3 Smith chart plot for lumped port conventional MSA

C) Incident and Reflected Waveforms

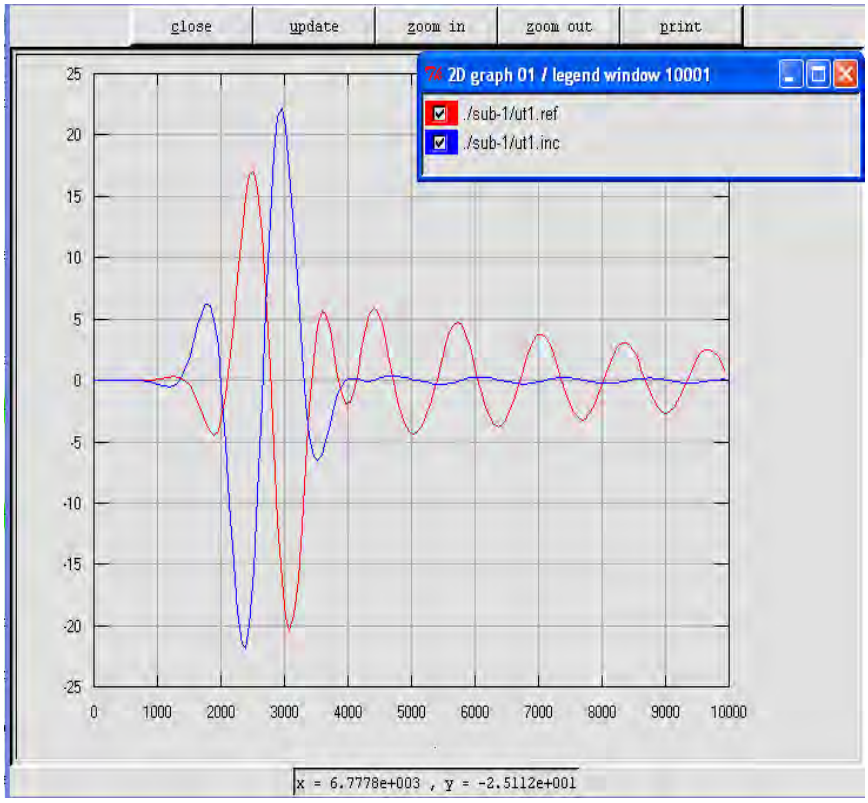

Fig 4.4 Incident and Reflected Waveforms for lumped port conventional MSA

Figure 4.4 above shows the incident and reflection wave

D) Input Impedance Curve

Figure 4.5 below is taken from the simulated output snap that shows the input impedance variation with frequency. As can be seen from the figure, around the desired resonant frequencies, the real part of the input impedance attains its maximum at 2.45GHZ and the imaginary part is minimum.

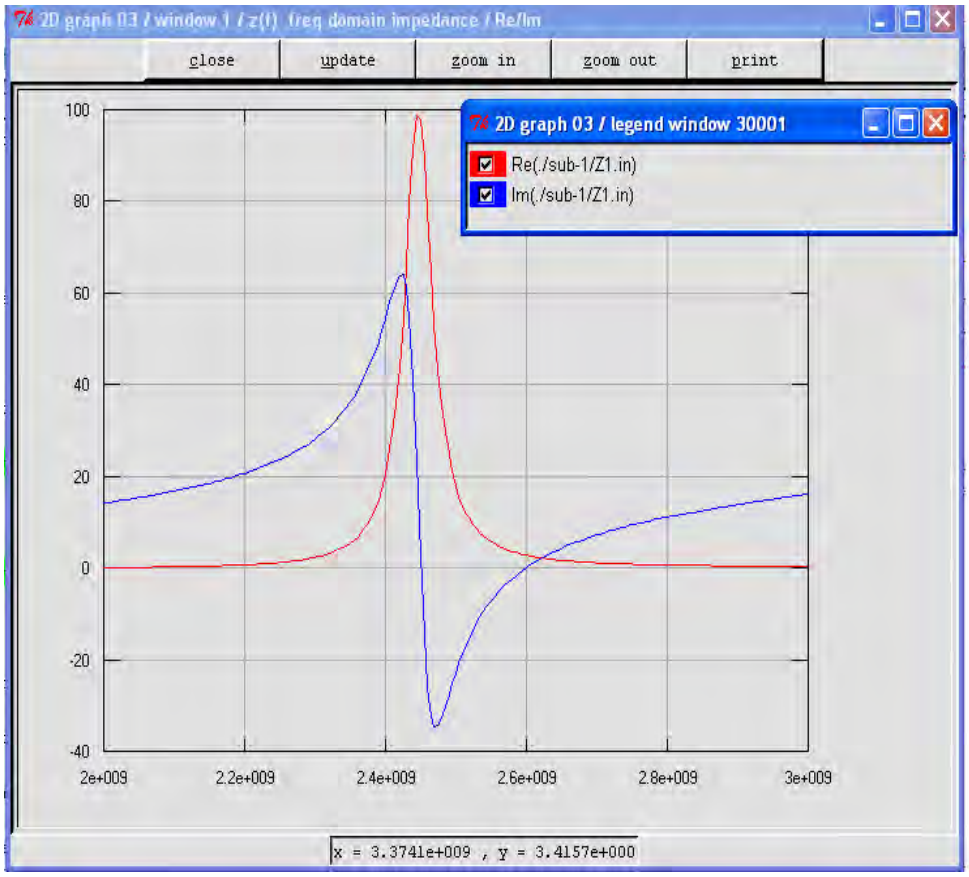

Fig.4.5 Input impedance curve for lumped port feed conventional MSA

E) Radiation Pattern Plots

A microstrip patch antenna radiates normal to its patch surface. Figure 4.6 below shows the 2D radiation pattern of the antenna at the designed frequency.

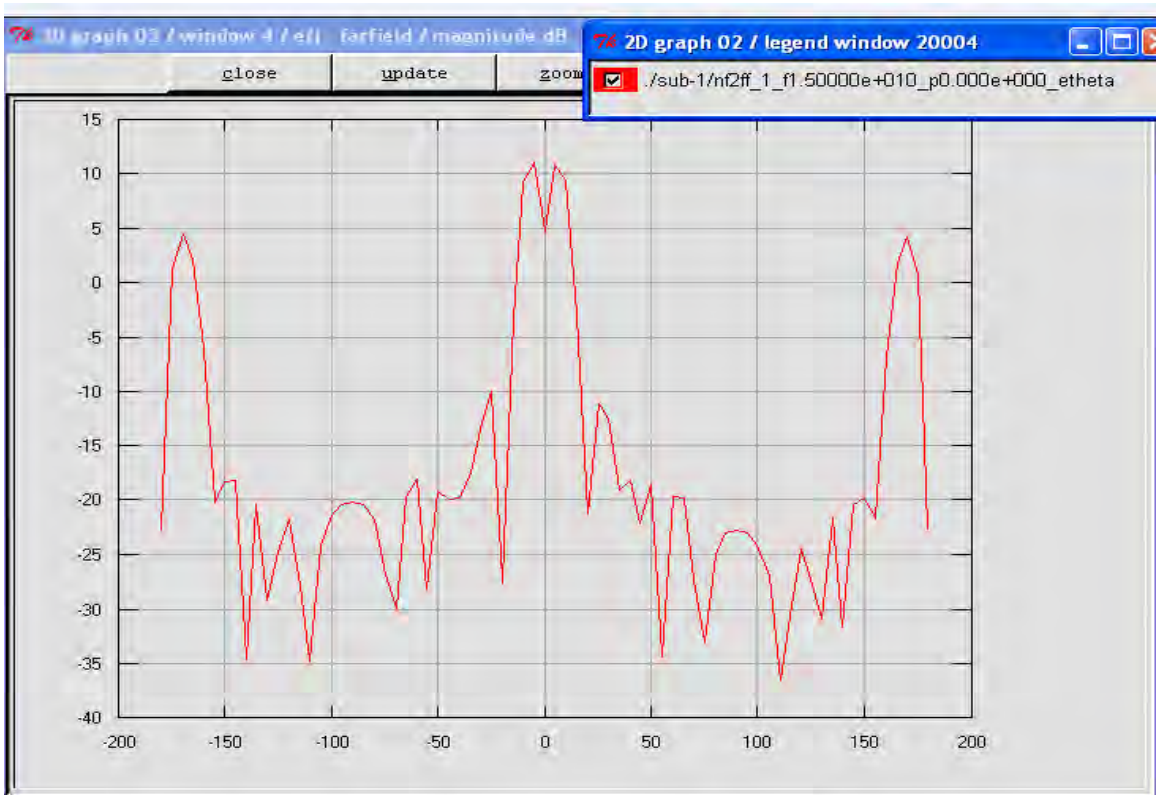

Fig.4.6) Far-field radiation pattern for lumped port conventional MSA

The radiation pattern plot of an antenna tells us the gain obtained at the respective operating frequency. It is a plot of the antenna gain versus the elevation angle. The antenna has a gain of 10dB at 2.45GHz

3D Plots

The maximum gain is obtained in the broad side direction. Figure 4.7below shows the snap taken from the animation of the three dimensional radiation pattern of the simulated results of lumped port feed conventional MSA at 2.45GHz the radiation pattern is somehow isotropic.

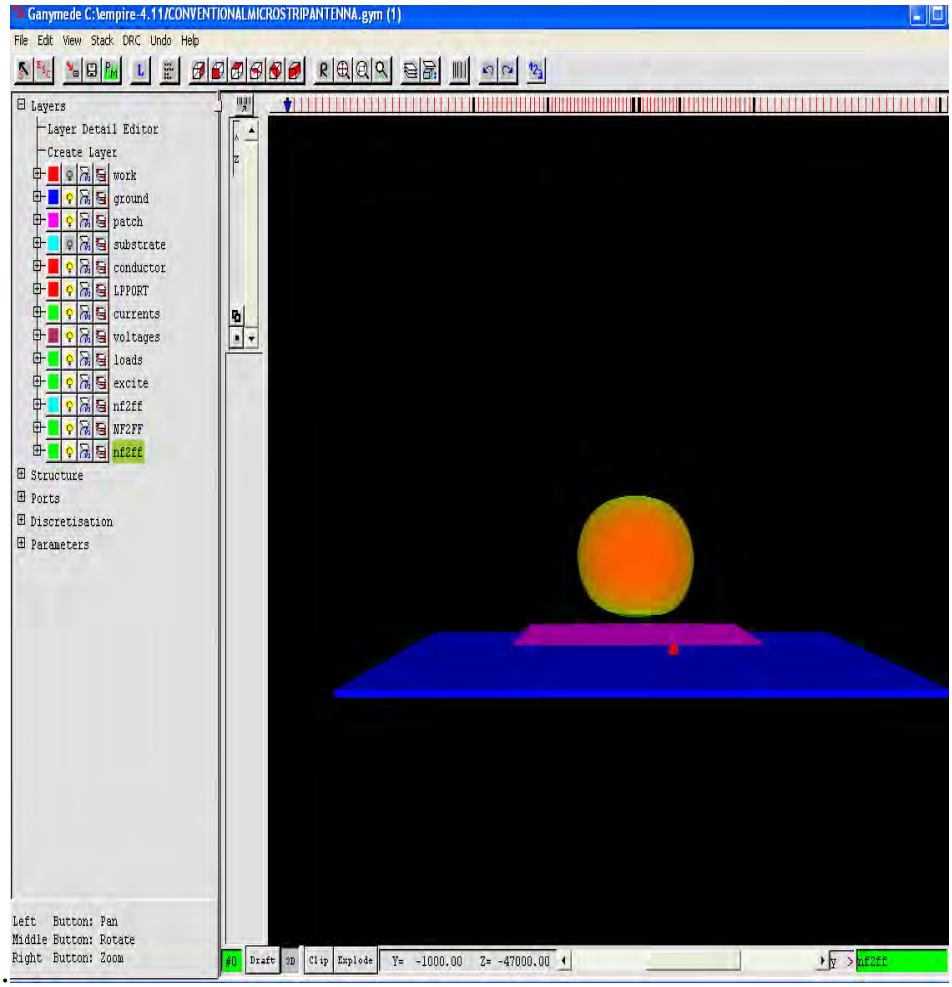

Fig.4.7 Radiation plot (3D) for lumped port conventional MSA

4.2) Lumped port feed Stacked Configuration Microstrip Antenna

The stacked antenna consisted of two layers, each patch antennas use four equal U shape on each sides of square microstrip patch antenna. Thus the effective size of the patches is reduced. The separation between the upper patch and the lower patch is 4.6mm and the separation between the lower patch and the ground plane is 7.2mm. The dielectric constants of the upper and lower substrates are 3.1 and 1.6 respectively.

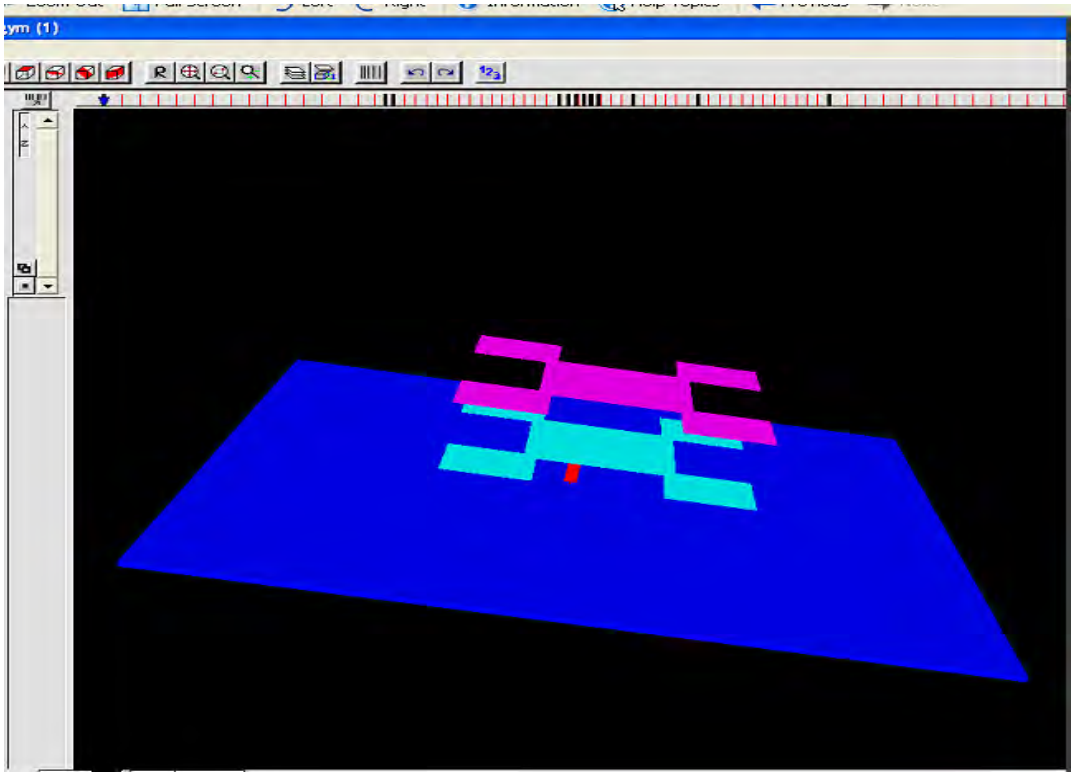

Fig.4.8 Physical structure of lumped port feed stacked microstrip antenna (3D).

Results

A). Return Loss (S11 Parameter)

The scattering parameter, S11 of the stacked configuration of microstrip antenna is given in Figure 4.9. It is better to measure the bandwidth at the lowest return loss (RL≤-9.5db or VSWR≤2.) Thus the antenna has almost 4.0GHZ resonance frequency and it has 2.2GHZ bandwidth at -12dB return loss (the difference of 3GHZ and 5.2GHZ)

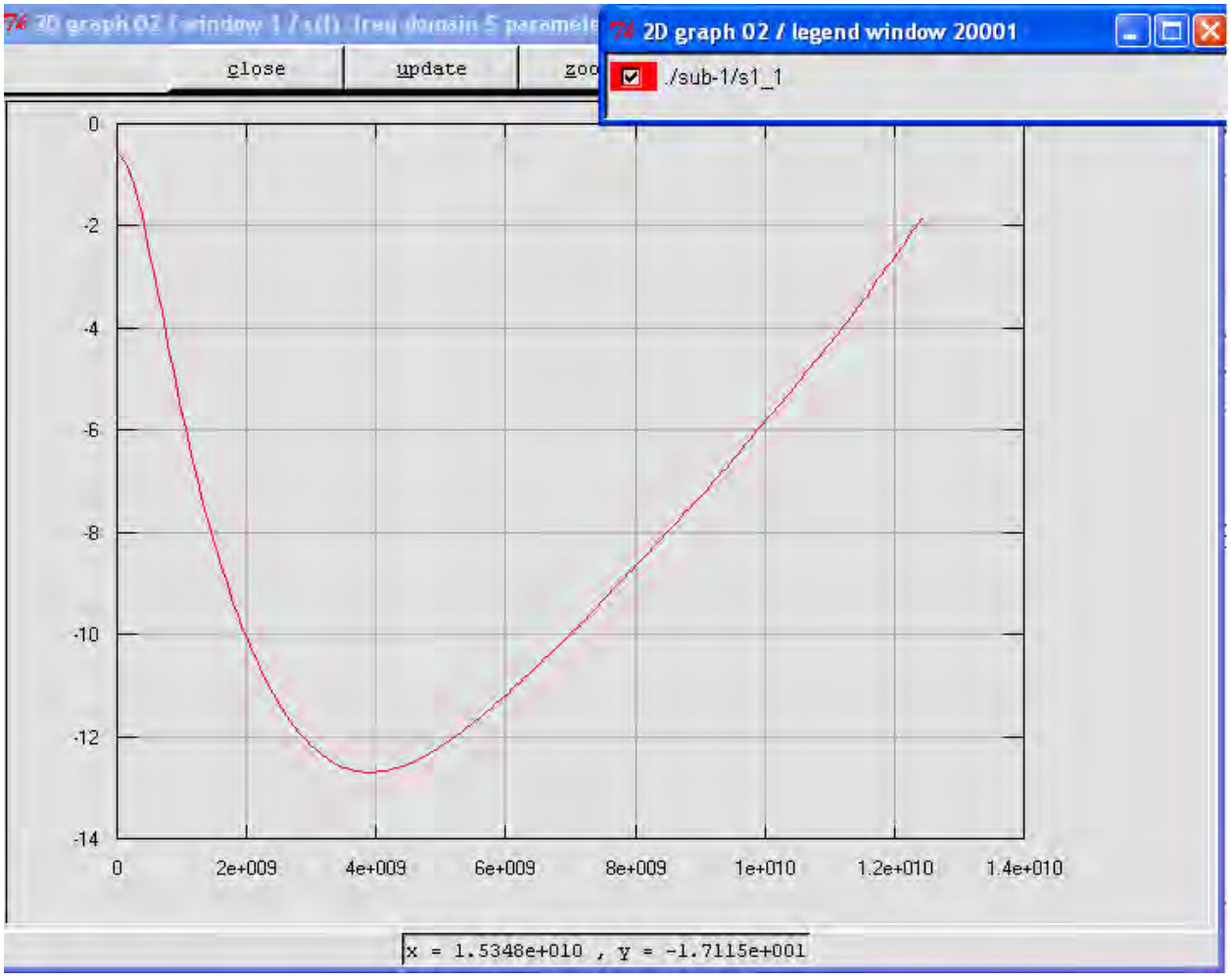

Fig.4.9 Return loss graph for lumped port feed stacked MSA

B) The Smith chart plot

The Empire simulator also provides smith chart plot of lumped port feed stacked microstrip patch antenna. The result indicates that the line impedance magnitude of the patch antenna intersects the unit circle of the smith chart in the frequency range of 1.8148 GHz–7.4667GHz. It crosses a unit circle, where the reflection coefficient| Γ | is zero, confirming no reflected power due to mismatching

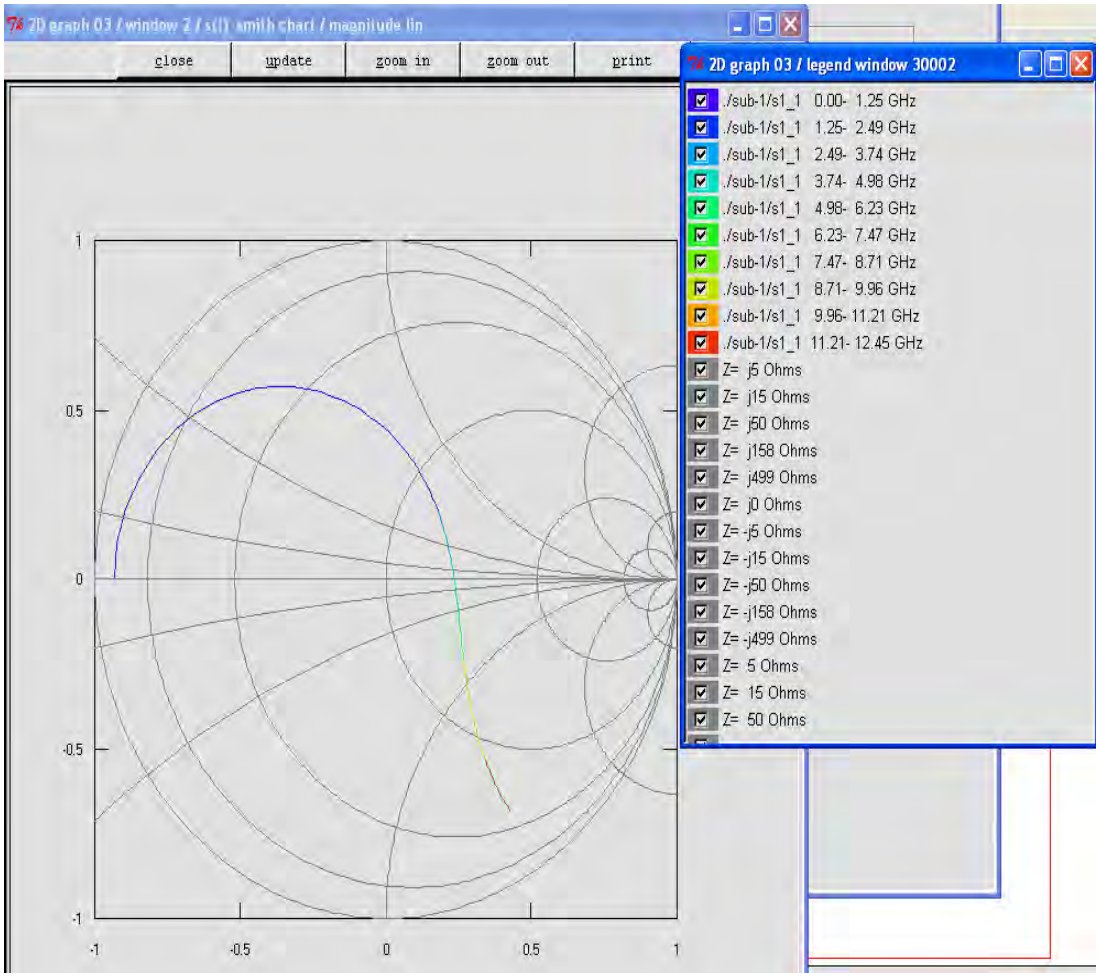

Fig.10.smith chart for lumped port stacked MSA

B) Input Impedance Curve

Figure 4.10 below shows the input impedance variation with frequencies. Around desired resonance frequency the real part of input impedance attains its maximum at 2.448GHZ and the imaginary part attains its minimum value.

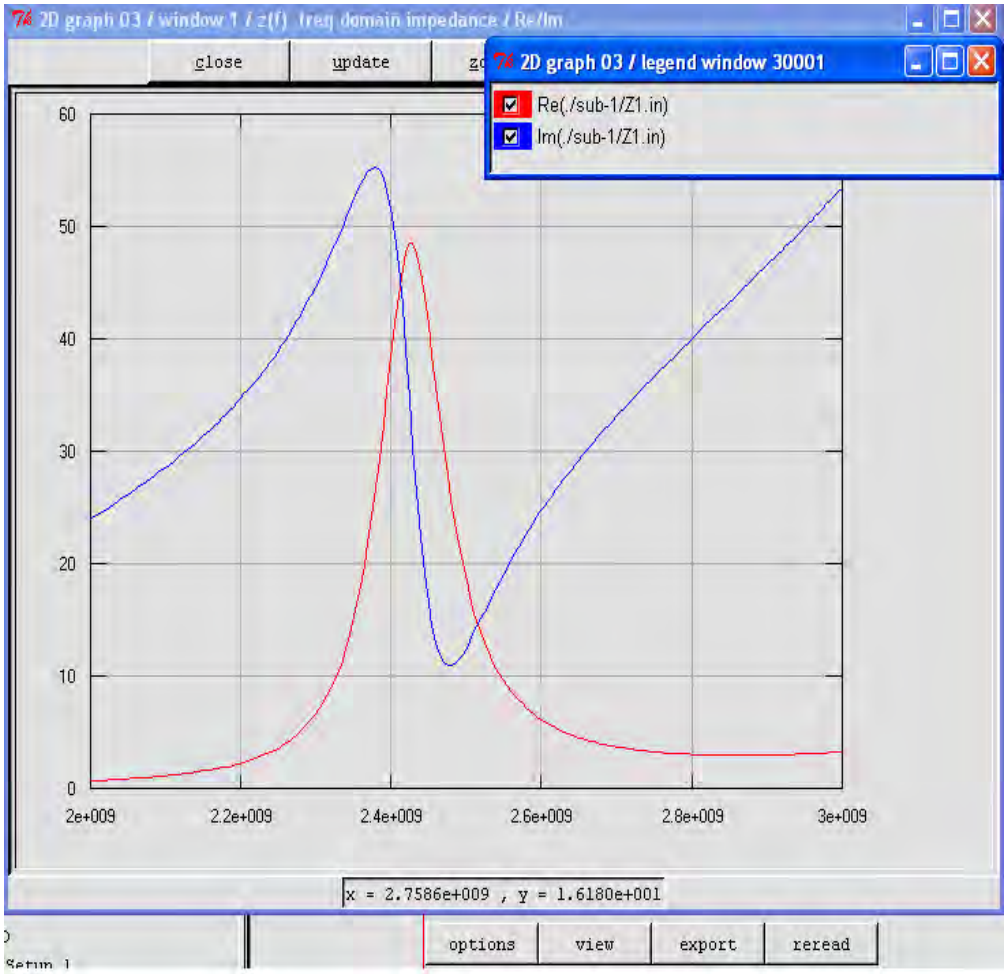

Fig.4.11.Input Impedance Curve for lumped port feed stacked MSA

C) Incident and Reflected Waveforms

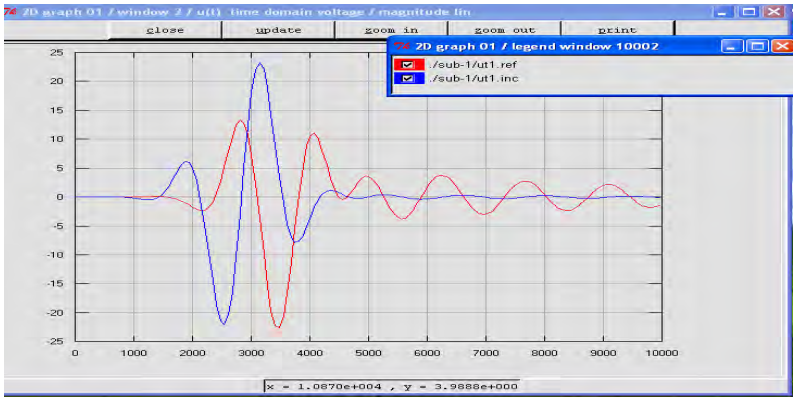

Fig.4.12 Incident and Reflected Waveforms for lumped port feed stacked MSA

Figure 4.11 above shows the incident and reflection wave

D.Fafieldradiationplot

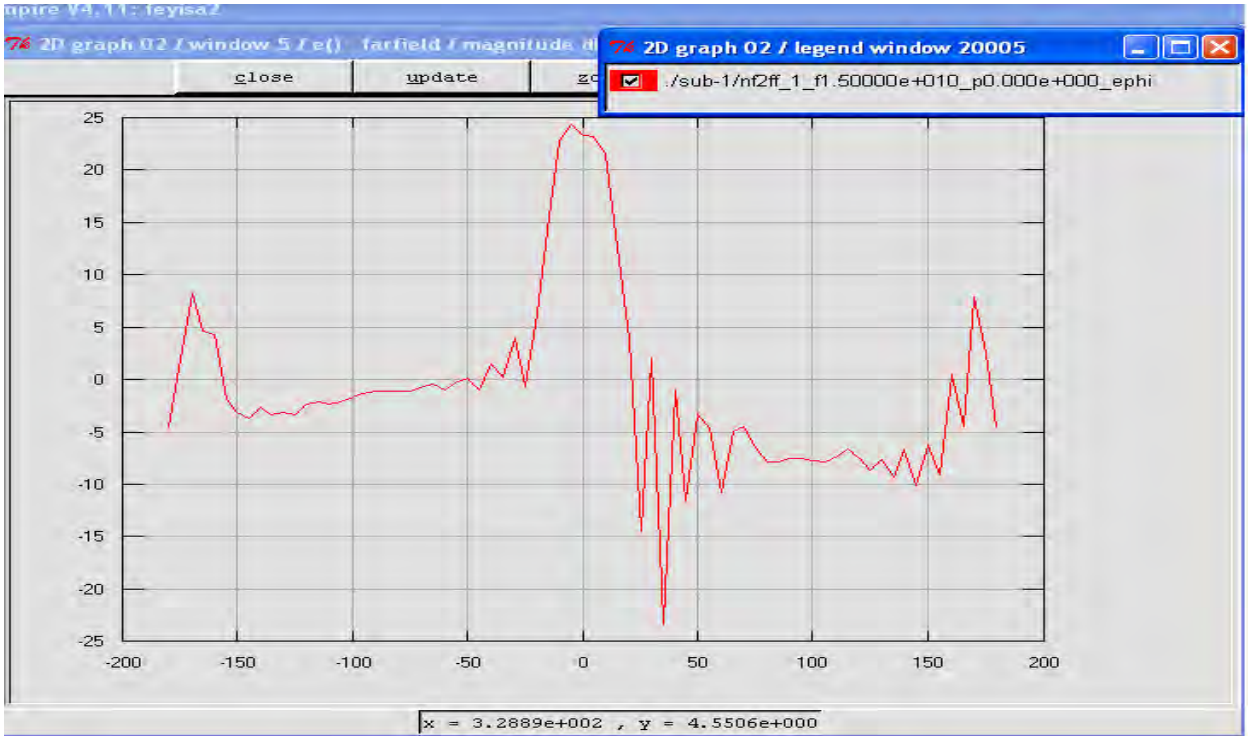

Fig.4.12) Far-field radiation pattern for lumped port feed stacked MSA

The radiation pattern plot of an antenna in figure 4.12 tells us the gain obtained at the respective operating frequency. It is a plot of the antenna gain versus the elevation angle. The antenna has a gain of 24dB at 2.48GHz as shown in the Figure 4.12.

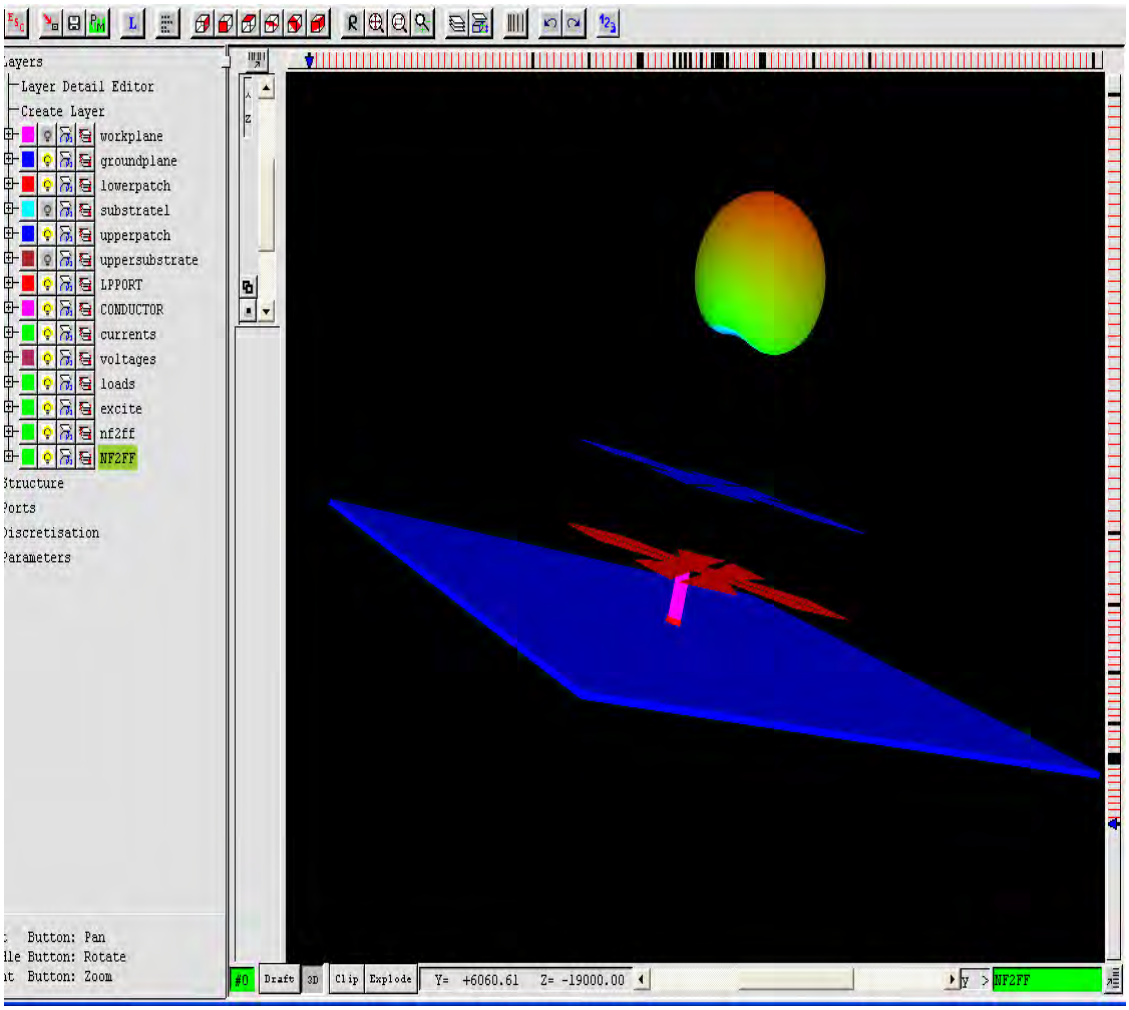

Fig. 4.13 Radiation of a stacked microstrip antenna (3D)

From the 3D radiation Pattern at 2.48GHz, the pattern is seen to be directive and it is almost isotropic.

4.3) *Microstrip Line Feed Conventional Microstrip Antenna*

Physical structure

Here a square microstrip patch of dimensions 2.82cmx2.82cm with dielectric substrate $_r$=4.4 and height of 0.16cm is fed with inset feeding method.

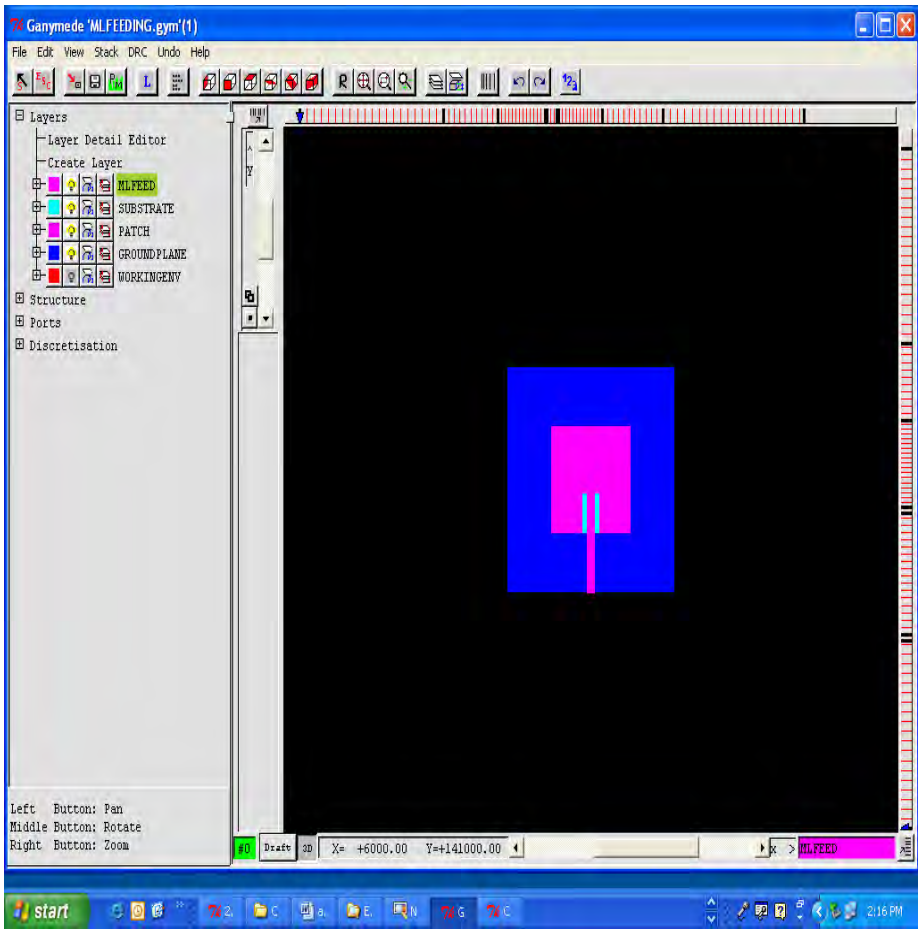

Fig.4.14 Physical structure inset feed conventional microstrip antenna

Results

A). Return Loss (S11 Parameter)

The simulated result of S11 scattering parameter of Conventional microstrip antenna is presented in Figure4.15. From the figure, the antenna has almost 2.45 GHZ resonant frequency and it has 38MHZ bandwidth at 9.5 dB return loss (the difference of 2.4754 GHZ and 2.4497 GHZ).

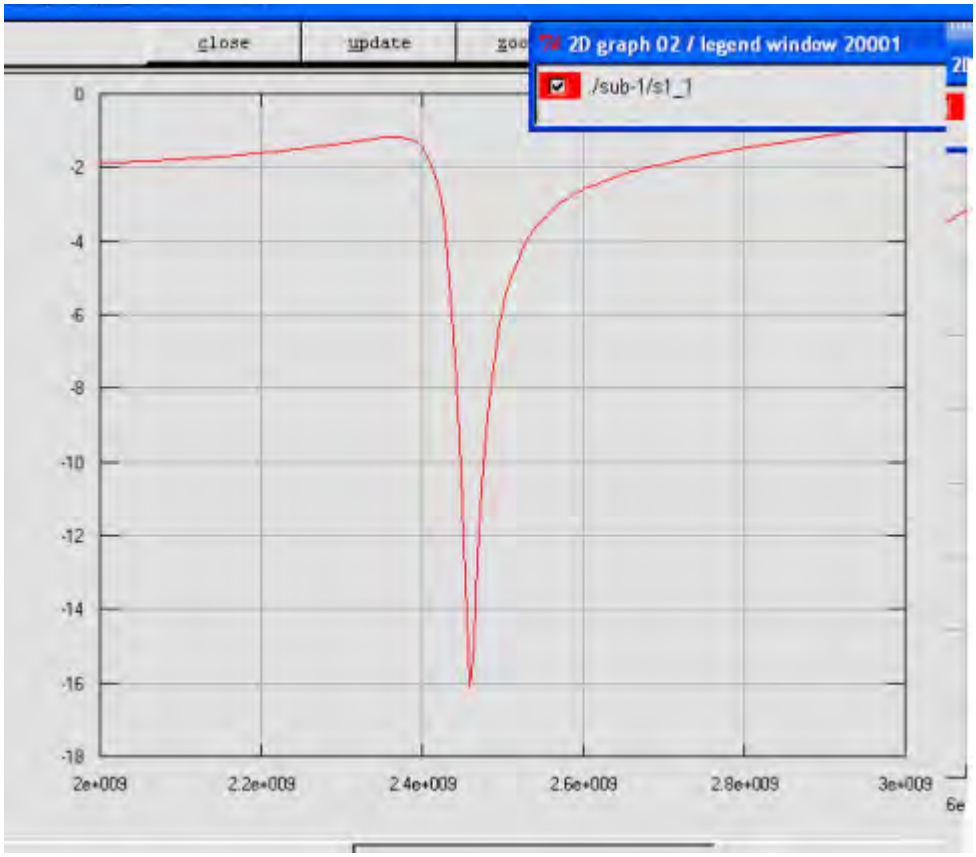

Fig.4.15 Return loss graph for inset feed conventional MSA

B) Input Impedance Curve

The real and imaginary component of input impedance as expected at resonance where the imaginary part is minimum and the real part is maximum as shown in figure 4.16.

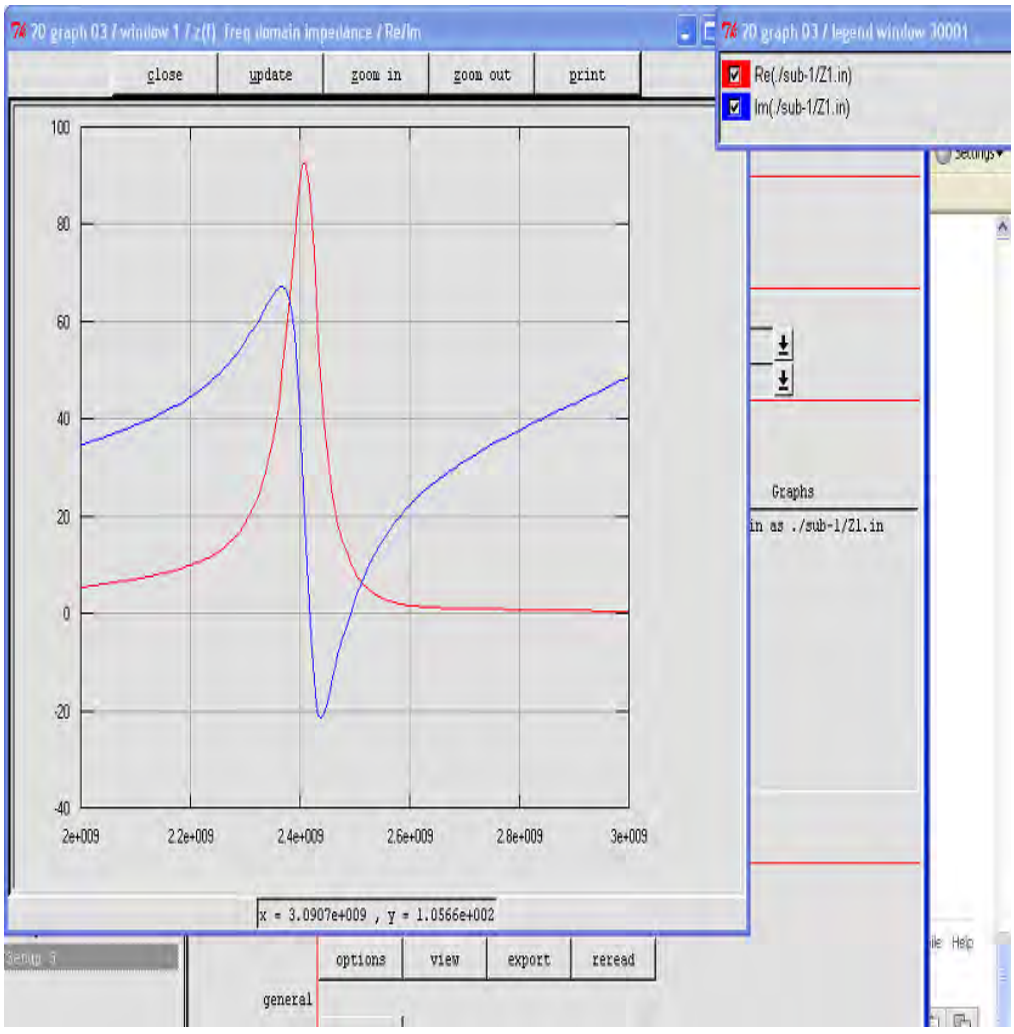

Fig.4.16 Input impedance graph for inset feed conventional MSA

C) Incident and Reflected Waveforms

Figure 4.17 below shows the incident and reflection wave

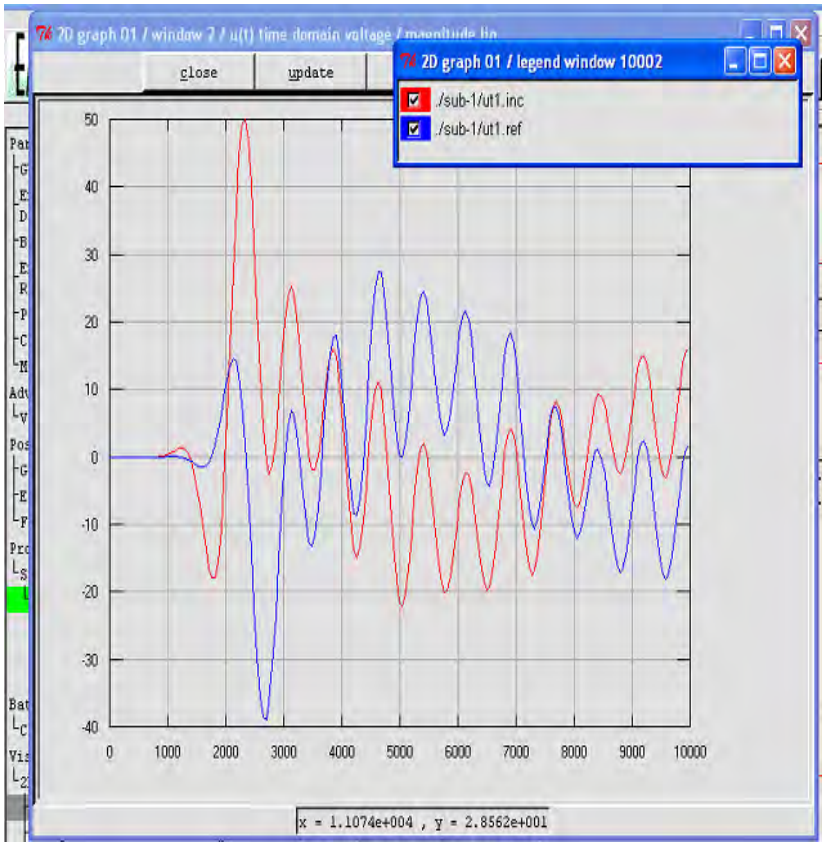

Fig.4.17 Incident and reflected wave form for inset feed conventional MSA

D) The Smith chart plot

The simulation shows (see Figure 4.18) that impedance lines of inset feed conventional microstrip patch antenna intersect the unit circle of the smith chart in the frequency range of 2.4754 GHZ -2.4497 GHZ. It crosses a unit circle, where the reflection coefficient $|\Gamma|$ is zero, confirming no reflected power due to mismatching.

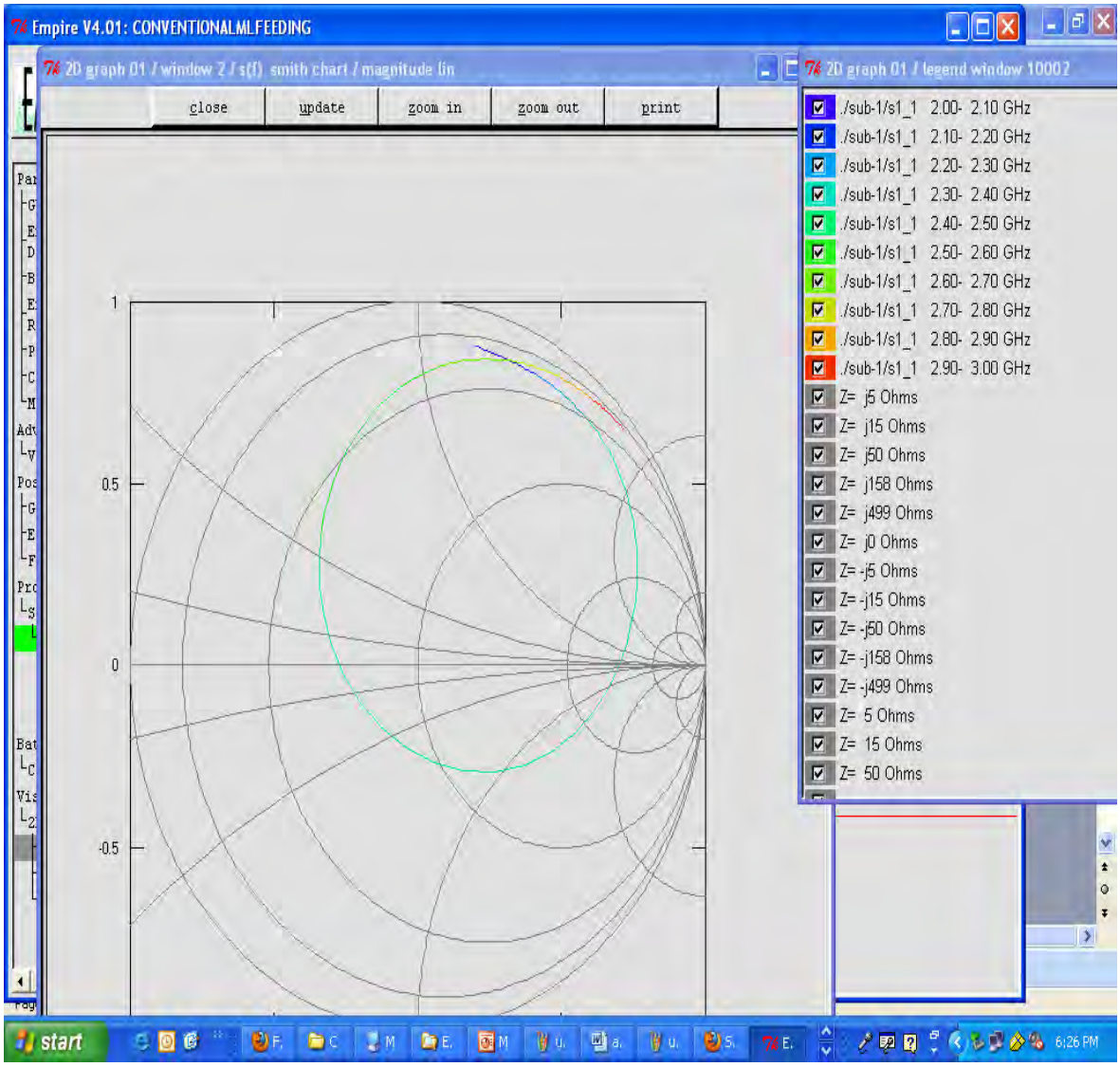

Fig.4.18 Smith chart graph for inset feed conventional MSA

E) Far field radiation plot

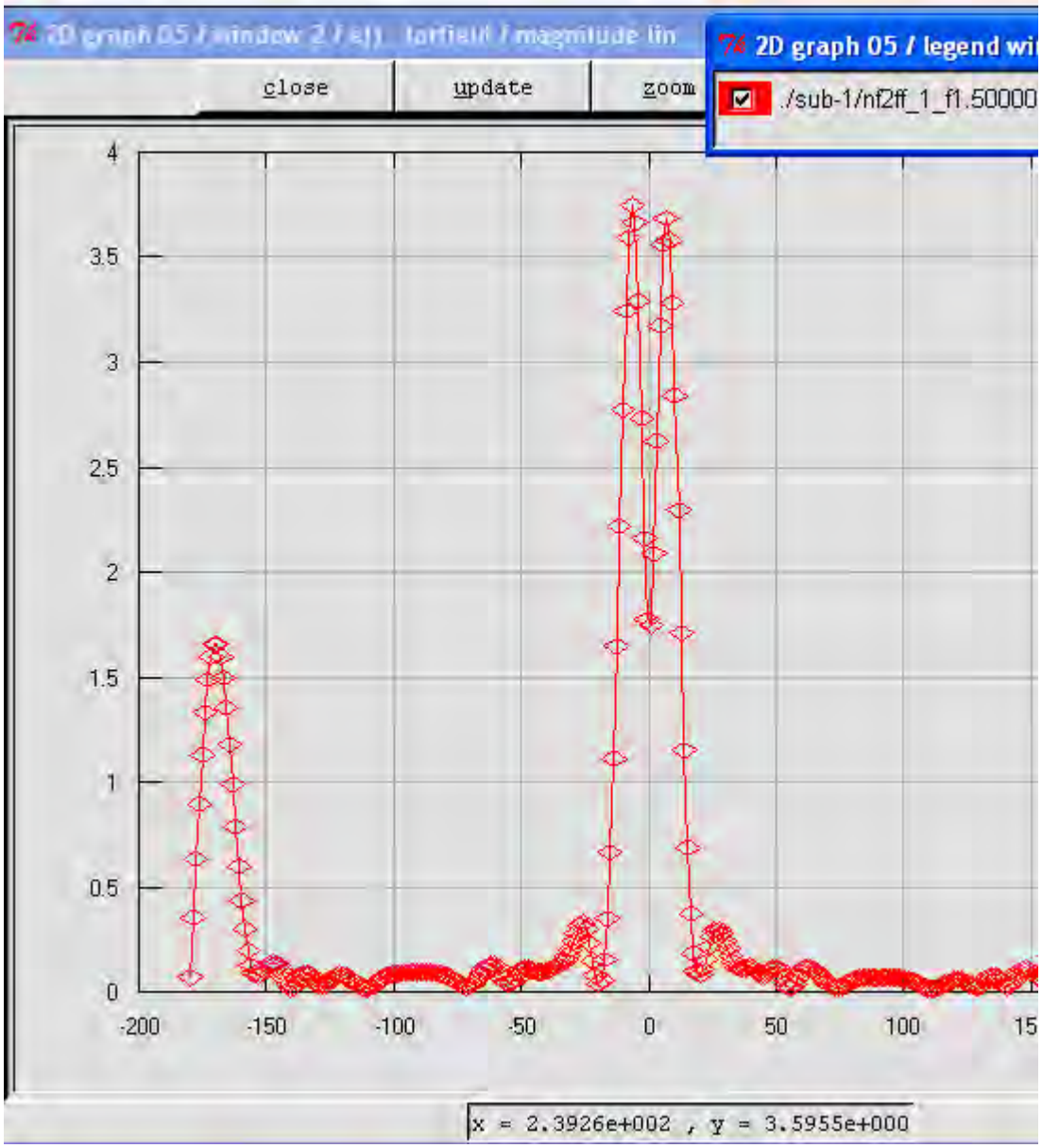

Fig. 4.19 Far-field radiation graph for inset feed conventional MSA

The radiation pattern plot in figure 4.19 above shows that the antenna has a gain 3.7dB at 2.45GHz.

4.4) Microstrip line Feed Stacked Layer Microstrip Antenna Physical structure

The stacked antenna consists of two layers. The patch antenna uses U-shape on four sides of each patch . Thus the effective size of the patches is reduced. The separation between the upper patch and the lower patch is 4.6mm and the separation between the lower patch and the ground plane is 7.2mm. The dielectric constants of the upper and lower substrates are 3.1and 1.6 respectively. Figure 4.20 below shows the configuration of inset feed stacked MSA.

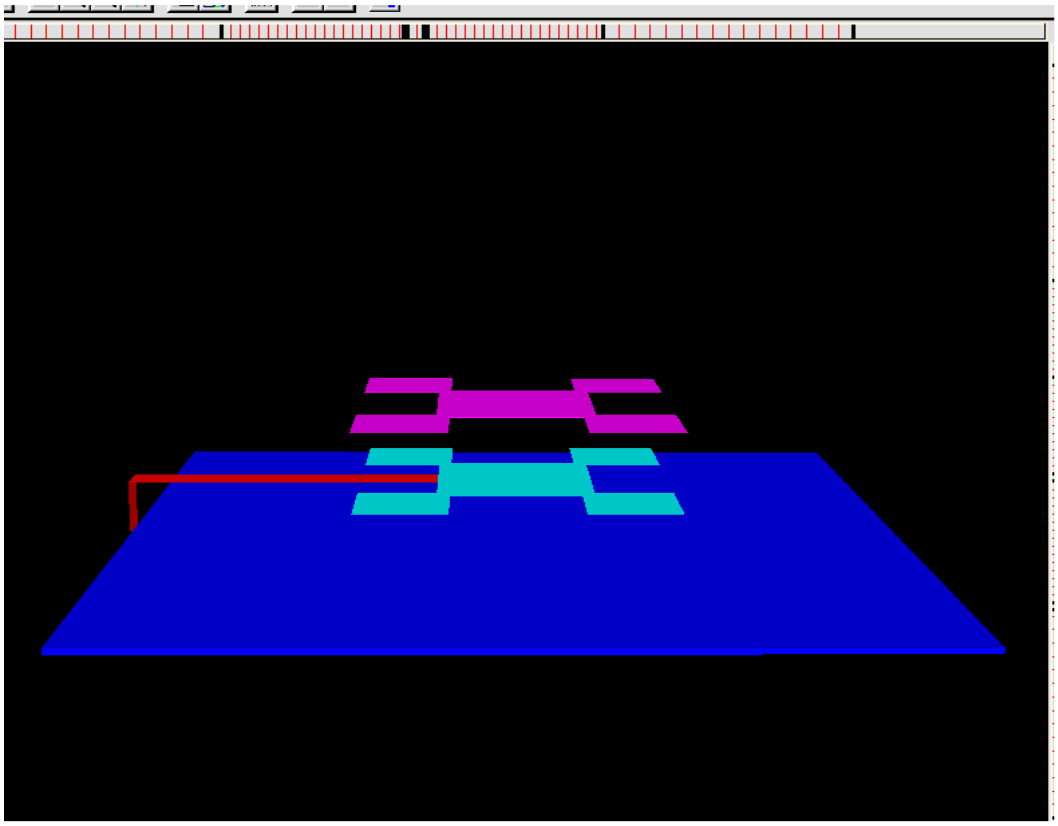

Fig.4.20 physical structure of inset feed stacked MSA.

A) . Return Loss (S11 Parameter)

The scattering parameter, S11 of the stacked configuration of microstrip antenna is given in Figure 4.21.The antenna has almost 2.46GHZ of resonance frequency and it has a bandwidth of 766.6MHZ at return loss of 9.5dB (the difference of 1.9556GHZ and 2.7222GHZ)

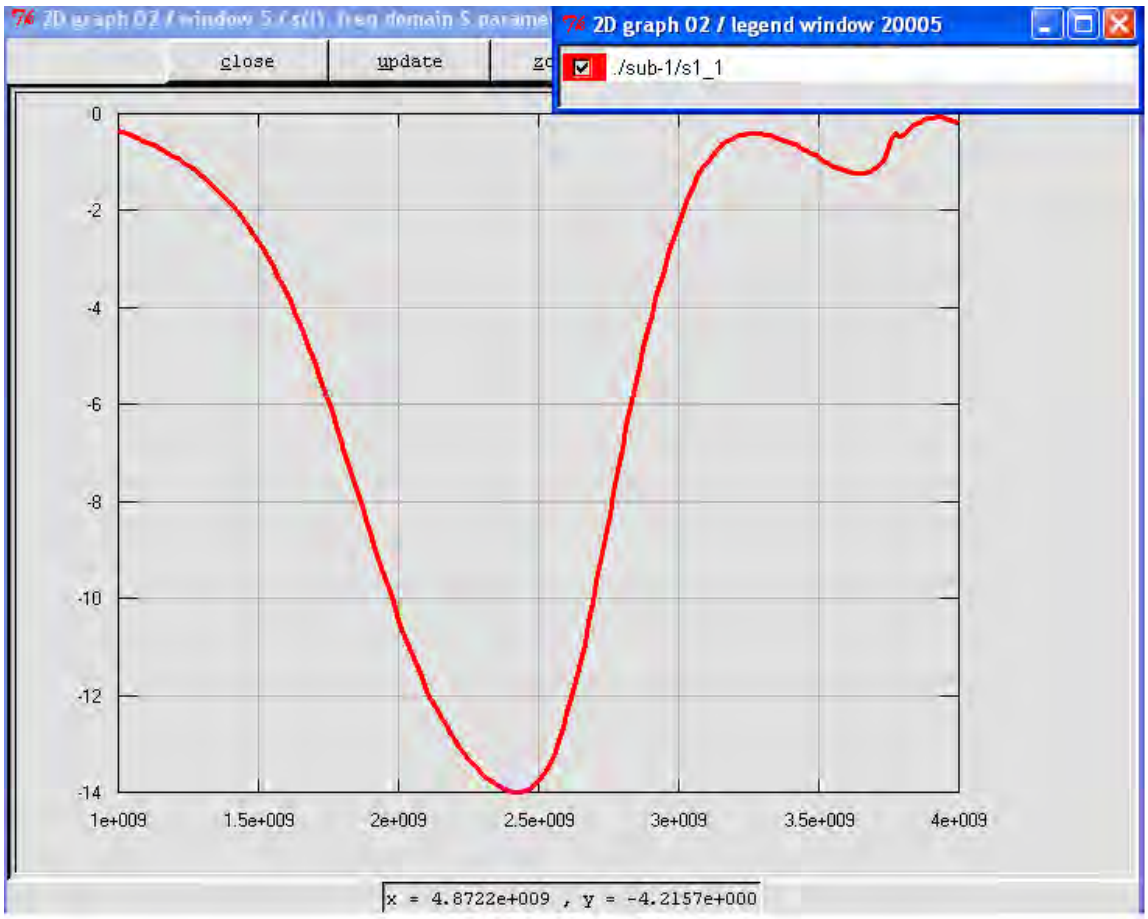

Fig.4.21 Return loss graph for inset feed stacked MSA

B) Input Impedance Curve

Figure 4.22 below shows that at resonance frequency the real part of input impedance is maximum, where as the imaginary part of input impedance is minimum.

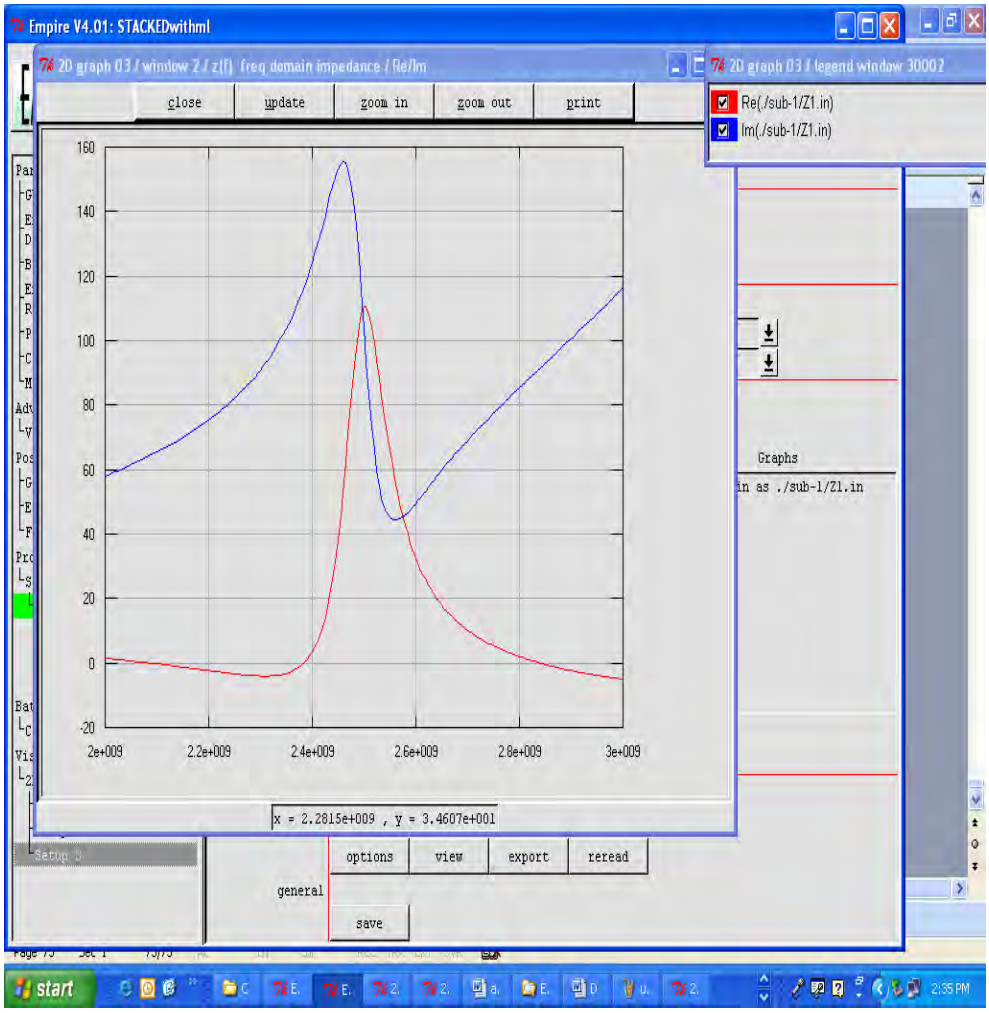

Fig.4.22 Input impedance graph for inset feed stacked MSA

C) Incident and Reflected Waveforms

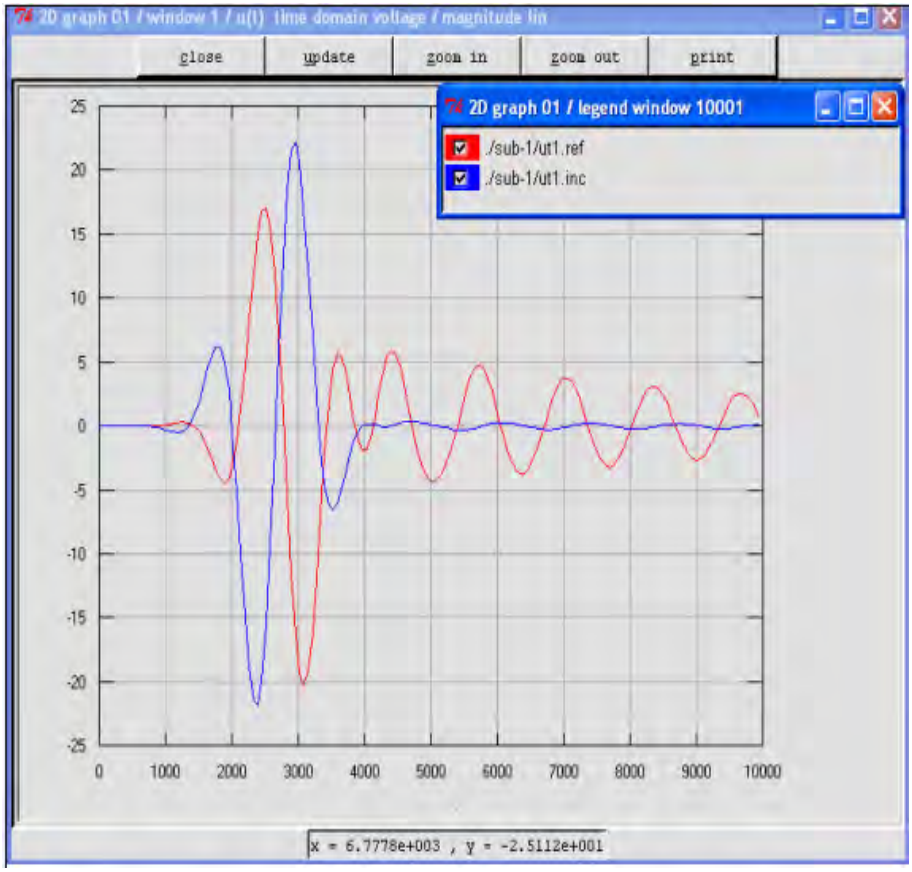

Fig.4.23 incident and reflected graph for inset feed stacked MSA

D) Far field radiation plot

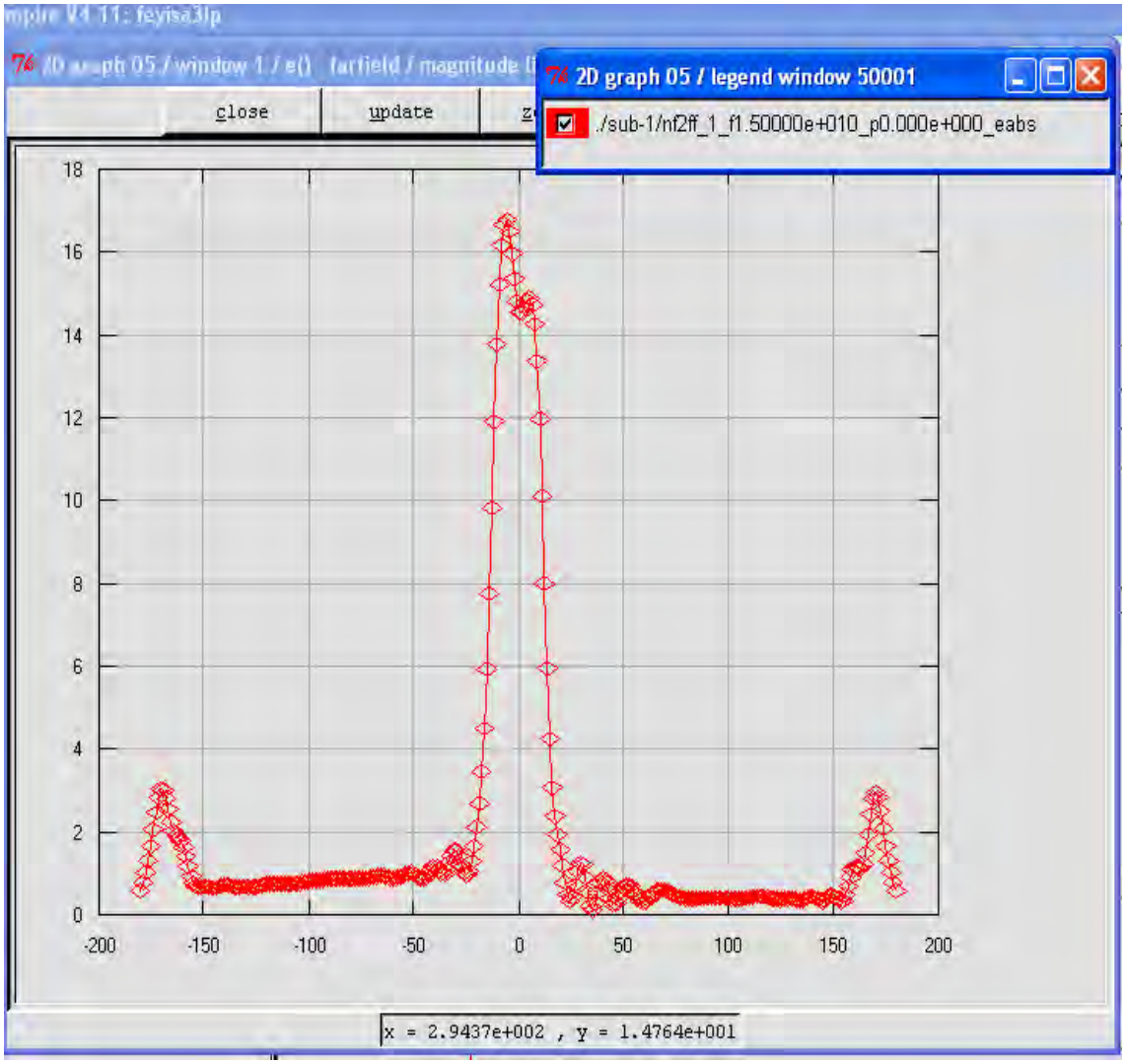

Fig.4.24 Far-field radiation graph for inset feed stacked MSA

Figure 4.24 above shows that the antenna has a gain of 16.3dB at operating frequency of 2.46GHz.

E) The Smith chart plot

The simulation shows (see Figure 4.25) that impedance lines of inset fed stacked microstrip patch antenna intersect the unit circle of the smith chart in the frequency range of 2.42 GHz_2.49GHz around operating frequency. It crosses a unit circle, where the reflection coefficient | Γ | is zero, confirming no reflected power due to mismatching.

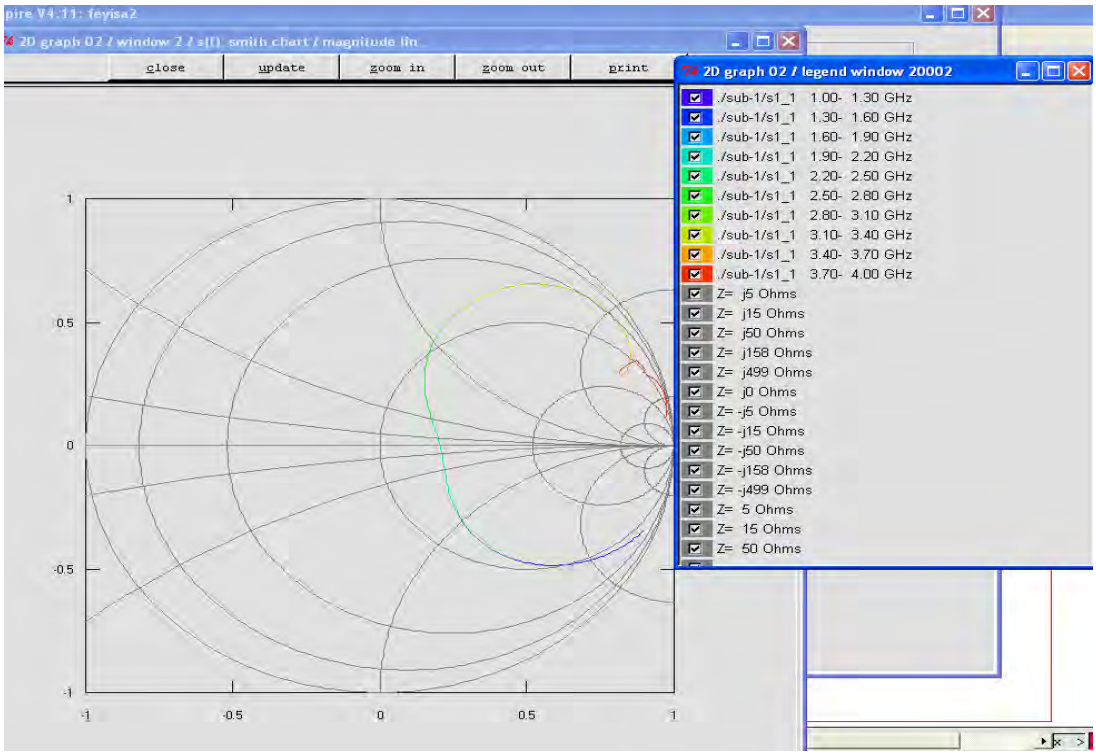

Fig.4.25 Smith chart graph for inset feed stacked MSA

4.5 Discussions

Based on the observations of simulation results, a performance comparison of conventional and stacked microstrip patch antennas with inset and lumped port feeding techniques are summarized in the table below.

Antenna types	*Bandwidth*	*Gain*	*Reduction in area*
Microstrip line feed conventional antenna	*38MHZ*	*3.7dB*	
Microstrip line feed stacked layer antenna	*766.6MHZ*	*16.3dB*	*70%*
Lumped port feed conventional antenna	*46.3MHZ*	*10dB*	
Lumped port feed stacked layer antenna	*2.2GHZ*	*24.4dB*	*70%*

Table 4.1 Performance comparison of conventional and stacked microstrip antennas.

CHAPTER 5

CONCOLUSIONS AND RECOMANDATIONS FOR FUTURE WORKS

5.1 Conclusions

In this thesis a conventional microstrip antennas and stacked layer microstrip antennas are designed, simulated and their performances are compared. Observations are made on the radiation pattern, return loss and input impedance. A microstrip line feeding and lumped port feeding techniques are introduced to feed the patches. Different types of feed methods affect the performance of an antenna. From the results it can be clearly seen that lumped port feeding technique has better performance than microstrip line feeding method in stacked configurations.

In order to reduce the area of microstrip patch antenna, the u-shape on four sides of each patch is used. One problem associated with this patch is diminished antenna gain and bandwidth. Stacked configuration design significantly improves the gain and bandwidth of the slotted patch.

One of the difficulty in the simulation process was getting the exact location of a feed since the exact location (which the

designer is convinced with) around some promising region is found by trial and error.

Another difficulty which is the most difficult one in designing patch antenna is maintaining all the antenna parameters at the desired level. For example while one searches for larger bandwidth the antenna gain may go down. If one needs a compact and size reduced antenna we should sacrifice the bandwidth.

The third challenge was to design slot patch on empire software since it is very difficult to cut the patch along the edges and diagonals.

Overcoming the above challenges, a compact microstrip antenna is realized in stacked configuration for WLAN application. The lumped port feed in stacked configuration enhanced both gain and bandwidth of the antenna in the 2.45GHZ operating frequency. A size reduction of 70% is obtained in the proposed configuration along with 24.4dB gain and 6.6519 GHz band width.

5.2 Recomandations for Future works

Further studies can be carried out in the following areas:

1) By increasing the distance between parasitic and feeding patch it is possible to design a dual or triple resonance stacked microstrip antenna with out loss of performance.

2) To reduce the antenna size by using dielectric substrates having higher dielectric constants and using a method of shorting posts.

3) Another area of interest is examining the effect of the ground plane dimensions on the performance of the antenna element in order to increase system performance.

REFERENCES

1. C.A. Balanis, Antenna Theory: Analysis and Design, John Wiley & Sons, Inc,1997

2. Kin-Lu Wong: Compact and Broad Band Microstrip Antennas, John Wiley & Sons, Inc, 2002

3. Two Compact Microstrip Patch Antennas for 2.4 GHz Band – A Comparison .vibha Rani Gupta and Nisha Gupta

4.Daniel Mamo," *Design and Simulation of Multiband Microstrip Patch Antenna for Mobile Communications."* September 2006 G.C, an MSc thesis.

5.Ehsan G. Doust,"An Aperture-Coupled Stacked Microstrip Antenna for GPS Frequency Bands L1, L2and L5." August 2007,MSc thesis.

6STEVEN S. HOLLAND," MINIATURIZATION OF MICROSTRIP PATCH ANTENNAS FOR GPSAPPLICATIONS." May 2008,MSc thesis.

7. R. B. Waterhouse, "Design of probe-fed stacked patches," *IEEE Trans. Antennas Propagat.* Vol. 47, pp. 1780-1784, Dec. 1999

8. Kumar, G. and Ray, K.P., Broadband Microstrip Antennas, Artech House, Inc,2003.

9. JR James & P S Hall, Handbook of Microstrip Antennas, Peter Peregrinus Ltd.,1989

10. Pozar, D. M.(1996). *A Review of Aperture Coupled Microstrip Antennas: History, Operation, Development, and Applications*, University of Massachusetts: Article review.

11. Microstrip Antenna Design Handbook, 1st edition, R. Garg, P. Bhartia, I.Bahl and A. Ittipiboon, Artech House Publisher, Norwood, 2001

12. GAIN AND BANDWIDTH ENHANCEMENT IN COMPACT MICROSTRIP ANTENNA Vibha Rani Gupta(1) and Nisha Gupta(2) *Birla Institute of Technology, Mesra, Ranchi-835215, INDIA, rch_vibharch@sancharnet* (2) As (1) above, but Email-g_nisha@lycos.com.

13.R. B. Waterhouse, "Small microstrip patch antenna," *Electron. Letters*, vol. 31, pp. 604–605, Apr. 1995.

14.Microstrip Antennas, The Analysis and Design of a Microstrip Antennas andArrays, 1st edition, David Pozar, Daniel Schaubert, IEEE Press, New York, 1995.

15. P. A. Tirkas and C. A. Balanis, "Finite-Difference Time-Domain Method forAntenna Radiation," IEEE Transactions on Antennas and Propagation, Vol. 40,No. 3, pp. 334-340, March 1992.

16.C. A. Balanis, Advanced Engineering Electromagnetics. New York: John Wiley and Sons, 1989.

17.Enge, P.; Misra, P., "Special Issue on Global Positioning System," *Proceedings of the IEEE*, vol.87, no.1, pp.3-15, Jan 1999.

18.Kai Chang, "RF and Microwave Wireless Systems", *John Wiley & Sons, Inc., 2000.*

19. Keith C. Huie, "Microstrip Antennas: Broadband Radiation Patterns Using Photonic Crystal Substrates", Thesis submitted to the Faculty of the Virginia Polytechnic Institute and State University in partial fulfillment of the requirements for the degree of MSc in Electrical Engineering Blacksburg, VA, 2002

20. Richard Q. Lee, Roberto Acosta, and J. S. Dahele, "Microstrip Antenna Array with Parasitic Elements", Prepared for the 1987 AP-S International Symposium sponsored by the IEEE Blacksburg, Virginia, June 15-17, pp. 1-6, 1987

21. Lu Wong, K (2003). *Planar Antennas for Wireless Communications.* Hoboken, N. J: John Wiley & Sons.2003.

22. Clarke, R. W. *Lecture notes and lab scripts.* University of Bradford,2004.

23. Mohd. Kamal bin A. Rahim. *Teaching Module, RF / Microwave and Antenna Design.* UTM,2002.

24. Haneishi, M., and Suzuki, Y. (2000). Circular polarization and bandwidth.In: Garg, R., Bharti, P., Bahl, I., and Ittipiboon, A. *Microstrip AntennaHandbook.* Artech House, Boston. 219

25. Raisert, J. H. *Antenna polarization application note.*

26. Ramirez, R. R. (2000). Single – Feed Circularly Polarized Microstrip Ring Antenna and Arrays. *IEEE Transactions on Antennas anpropagation. Vol.*48,No 7, pp 1040 – 1047

27. Li, Q., and Shen, Z. (2002). An Inverted Microstrip – Fed Cavity – backed Slot Antenna for Circular Polarization. *IEEE*

Antennas for Wireless propagation letters. Vol.1,pp 190 – 192

28. Lu Wong, K (2003). *Compact and Broadband Microstrip Antennas*. Hoboken, N. J: John Wiley & Sons.

29. Dafalla, Z. I., Kuan, W. T. Y., Abdel Rahman, A. M., and Shudakar, S. C.(2004). Design of a Rectangular Microstrip Patch Antenna at 1 GHz. *2004 RF and Microwave Conference*. October 5 – 6: pp. 145 – 149

30. Setian, L. (1998). *Practical Communication Antennas with Wireless Applications*.Upper Saddle River, NJ: Prentice Hall

31. LEE. R. Q., LEE, K.F., and BOBINCHAK, J.:' Characteristics of a two-layer electromagnetically coupled rectangular patch antenna ', Electronic Letters.Vol.23,No.20,1987, pp. 1070-1072.

32. LEE, R. Q.. and LEE, K.F.:' Gain enhancement of microstrip antennas with overlaying parasitic directors ', Electronic Letters.Vol.24,No 11, 1988, pp. 656-658.

33. DAMIANO, J.P., BEMVEGUEOUCHE, J., and PAPIERNLK, A.:' Study of multilayer microstrip antennas with radiating elements of various geometry', IEE Proc. Vol=137, pt.H, No.3, June 1990, pp. 163-170.

34. BHATNAGAR., P. S., DANIEL, J.P., MAHDJOUBI, K., and TERRET, C.:'Experimental study on stacked triangular microstrip antennas'. Electronic Letters. Vol.22,No. 16, 1986, pp. 864-865.

35. BHATNAGAR., P. S., DANIEL, J.P., MAHDJOUBI, K., and TERRET, C.:'Displaced mutilayer triangular elements widen antenna bandwidth ', Electronic Letters.Vol.24, No.15, 1988, pp. 962-964.

36. LEE, C. S., NALBANDIAN, V , and SCHWERMG, F.: 'Planar Dual-Band Microstrip Antenna', IEEE Trans., Ap=43, No.8, August 1995, pp. 892-897.85

37. CROQ, F., and POZAR, D. M.: 'Multifrequency Operation of Microstrip Antennas Using Aperture Coupled Paralle1 Resonators', IEEE Trans., AP=40, No.11, Nov. 1992, pp. 1367- 1374.

38. WANG, B. F., and LO, Y. T.: 'Microstrip Antennas for Dual Frequency Operation', IEEE Trans., AP=32, No.9, Sept. 1984, pp. 938-943

39. K. Hirisawa and M. Haneishi, Analysis, Design, and Measurement of Small land Low-Profile Antennas, Artech House, Boston: 1992.

40. SANCHEZ-HEWANDEZ, D. and ROBERTSON, D.I.: ' Triple band rnicrostrip parch antenna using a spur-line filter and a perturbation segment technique ', Electronic Letters.Vol. 29,No 17,Aug. 1993, pp. 1565-1566

41. A New Compact Size Microstrip Patch Antenna with Irregular Slots for Handheld GPS Application, 5/9/2007

42.FRACTAL-SHAPE SMALL SIZEMICROSTRIP PATCH ANTENNA, *January 2002*

Appendix

Overview of Empire simulator

The EMPIRE™ simulator (ElectroMagnetic field simulator for the analysis of Packages, Interconnects, Radiators, Waveguide Elements) is a tool for solving Maxwell's equations, especially for radio frequency (RF) applications. It is based on the Finite Difference Time Domain method (FDTD), which means that the equations are discretized in space and time. This is accomplished by mapping the structure of interest onto a rectangular grid where the unknown field components are located in each cell.
Because of the nature of the electromagnetic problem, an initial value problem has to be solved. This means that the unknown field for a certain time is calculated from the field values before. The FDTD method employs an efficient time stepping algorithm, known as the Yee's leapfrog scheme shown in figure (A) below to solve the initial value problem. The size of the time steps is related to the size of the grid for stability reasons. So the definition of a suitable grid is an important task for efficient simulation.
The duration of a simulation run is proportional to the number of time steps needed. It strongly depends on the quality factor of the system, which can not easily be determined.

Finite Difference scheme discretizes the structure into cells in which the material properties are constant. These cells are formed by intersecting planes of a Cartesian co-ordinate system. The basic idea of the algorithm is to place the unknown field components in a certain position of each cell so that every electrical field component is surrounded by four circulating magnetic field components as shown in Figure A, and approximate Maxwell's differential equations

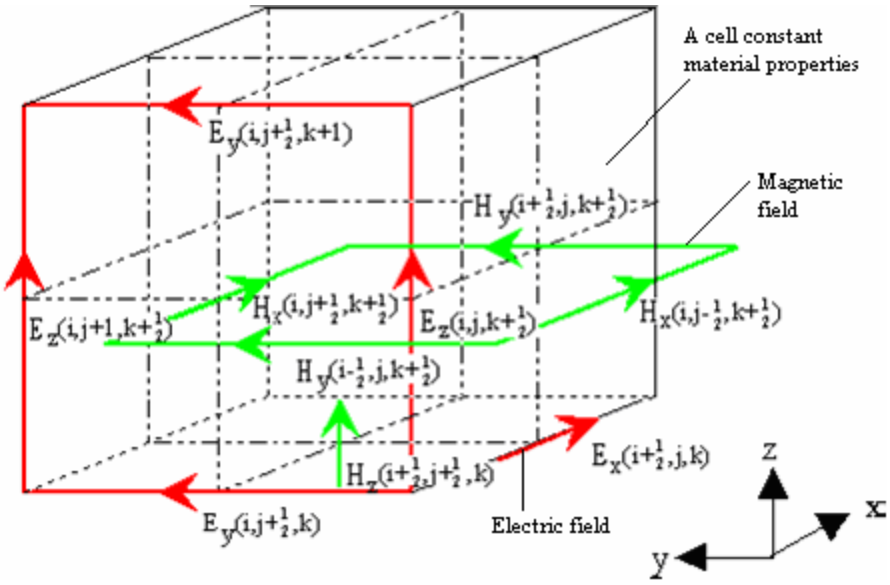

Figure A. Empire simulator and Finite Difference scheme

Application areas of the Empire simulator are listed below:

- Planar and multi-layered circuits including layout synthesis
- Microwave passive components
- MEMS switches
- Package simulation and modeling
- Antenna design and investigation
- Waveguides of arbitrary shapes including higher order modes
- EMC including safety considerations employing anatomical body models
- Mono- and bi-static scattering cross section calculation
- High quality structures including accurate loss modeling

Creating objects

1.1 setting prefences

It is assumed that the Ganymede icon is installed on the desktop of the PC or the EMPIRETM software is installed correctly on a workstation, e.g. the command empire is known.

Step 1: double click the Ganymede icon

If the installation set-up was done successfully, the Ganymede window as displayed in figure A.1 Empire to start.

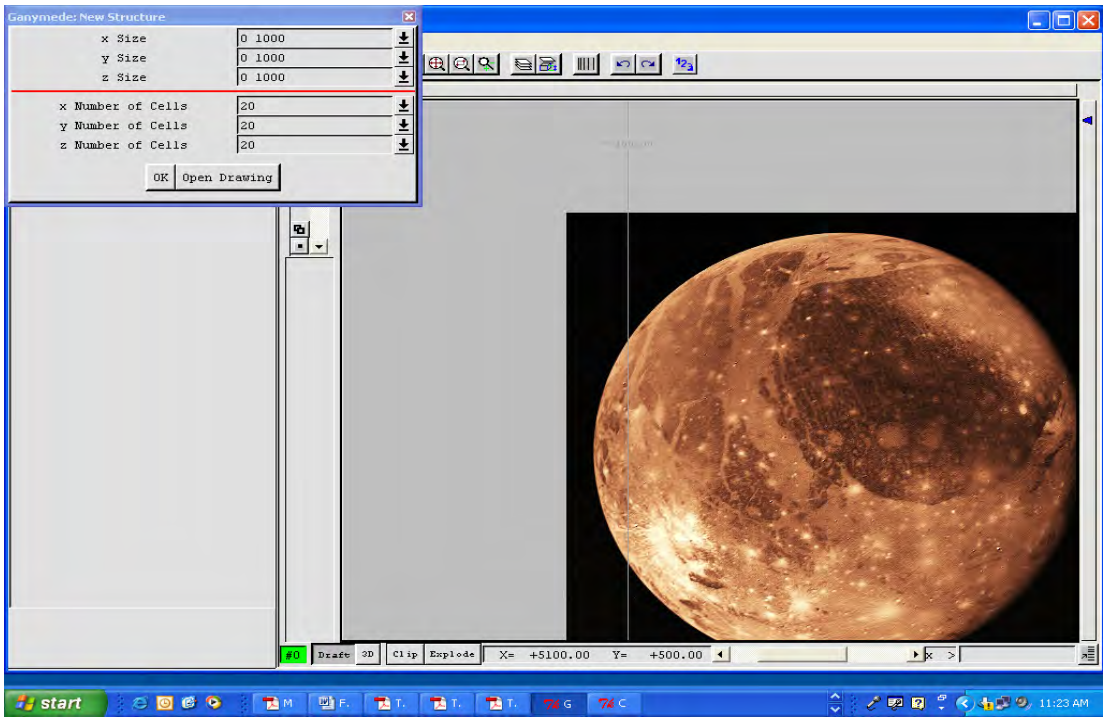

Figure A.1 Ganymede window

Step 2: creating the drawing area

Enter the size of structure: X0, Y0, Z0 and X1, Y1, Z1

Enter the basic discretization:

Press ok

As can be seen in the discretization bars, bold lines mark the entered

boundaries. The blue triangles mark the origin, black lines are fixed, red lines are un-fixed grid lines. The cross-hair cursor displays the current co-ordinate values, as shown figure A.2 after entering drawing area.

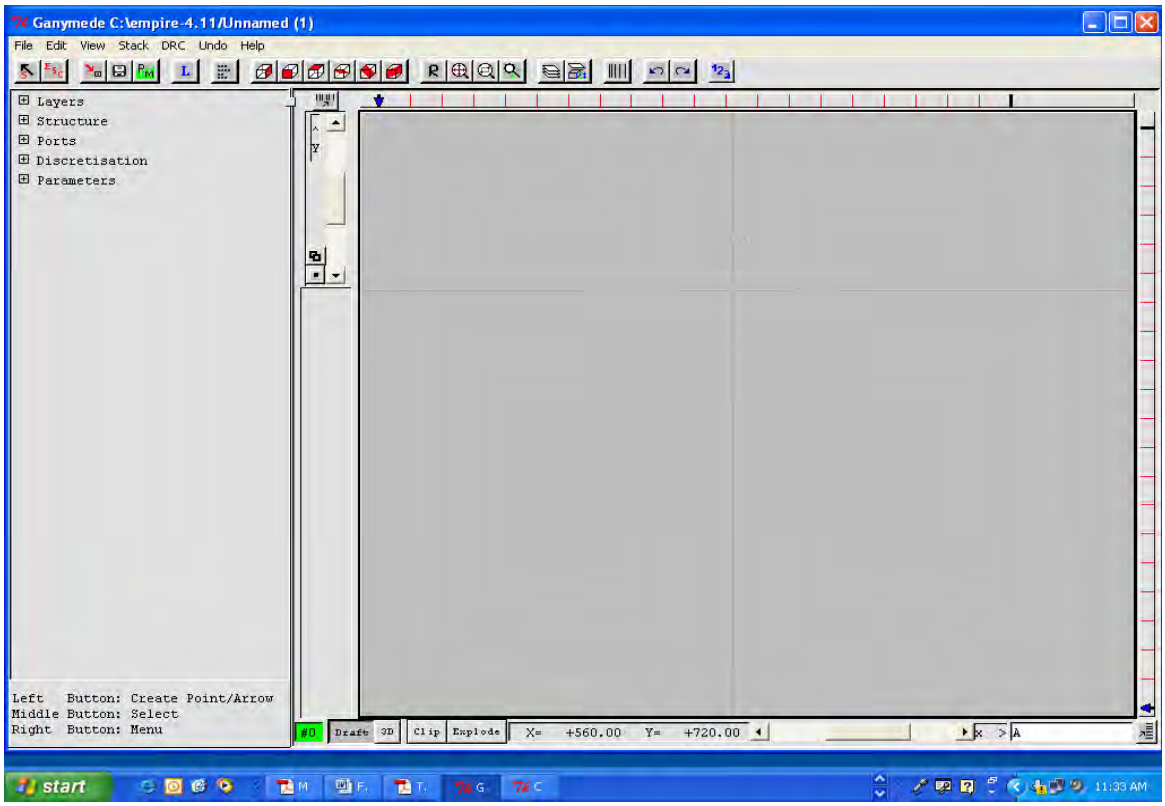

Fig.A.2 Discretization bars

Save Settings: file save as

Create the project directory C:\empire-data\tutorial using and select the new folder.

1.2 Creating and defining layers

Each object that will be created needs a layer and its property has to be defined.

1. Press Layers Create Layer on the left list.
2. Press sign of the newly created layer metal200

Then other properties like: material property, metal property etc can be defined. Once we know how to create layer and define its properties the next thing is discussing how to create objects like boxes, discs, cylinders, curved objects and slotted objects.

Note: In using this software after writing text or numbers we have to press the enter button on the keyboard. If not we will get the default value.

1.3 Defining Structures

Step1: double click the Ganymede editor

Step2: Enter the x, y, z size and the respective number of cells

Step 3: Press the OK button

Step 4: Press the Layers (a default layer named A is created)

Step 5: Optionally change layer's color or name

Step 6: Press metal 200 Object Definition General Objects

Material object

- ✓ Relative permittivity 1
- ✓ Conductivity 0
- ✓ Priority 100
- ✓ Tangent delta none
- ✓ Frequency for tangent delta in Hz 1e9

Step 7: Press the OK button

Step 8: Press Structure create box

1.4 creating a por

Step 1: Press the Layers (a default layer named A is created

Step 2: Optionally change layer's color or name

Step 3: press –port-create (chose the options)

1.5 Descretization

Step 1: Press the Top View button

Step 2: Press the left top square button with diagonal arrow

Step 3: Press Empty Descretization that is appeared at the left margin

Step 4: Select the port using middle mouse button and press the left top corner square button with diagonal arrow

Step 5: Press the Propose Discretization Local button

Step 6: Along the width of the object fix by pressing on the top descretization bar using Alt + left click

Step 7: Press on the empty gray space along the width

Step 8: Write frequency and dielectric constant on the key board and press the enter key.

Automatically you will see discretization.

The descretized 2D and 3D views are as follows. We have to note that during the 3D view the surrounding layer and the casing layers should be turned off and later turned on for simulation.

1.6 Simulation Procedure

Step 1: Press the Export & Save button close

Step 2: Press the Start Simulation button

Step 3 : Enter center frequency , Bandwdth, start ,stop

Step4: Press End Criteria-Resonance Estimation Switch ON -

Order of the mAvg system 40

Step 5: Press cleanup setup-cleanup selector (select all)

Step 6: Press Processing Start-complete simulationyes

Now the simulator starts to run.

Step 7: Press the Visualization setup 2

1.7 Post Simulation Process

- Create a new layer
- Change name to nf2ff (near feild to far field)
  - ✓ Press metal
    - ❖ Near field to far field transformation. set number of transformation in such away that the interested frequency will be obtained.
  - ✓ Press ok
  - ✓ Select post processing
    - ▪ Far field on the left list
    - ▪ Select far field calculation on the right list
  - ✓ Deselect all frequencies except the operating frequency
  - ✓ Press the save bottom on the top to save the far field settings.

Declaration

I, the undersigned student, declare that this thesis work is my original work, has not been presented for a degree in this or any other universities, and all sources of materials used for the thesis work have been fully acknowledged.

Name: Feyisa Debo Signature: _____

Place: Addis Ababa

Date of submission: April, 2010

This thesis has been submitted for examination with my approval as a university advisor.

Dr. Ing. Mohammed Abdo Signature: _____
Advisor's Name